JOURNAL OF GEOPHYSICAL RESEARCH, VOL. 93, NO. B5, PAGES 4797–4819, MAY 10, 1988

Late Neogene and Quaternary Tectonics Associated With Northward Growth of the San Andreas Transform Fault, Northern California

HARVEY M. KELSEY

Department of Geology, Western Washington University, Bellingham

GARY A. CARVER

Department of Geology, Humboldt State University, Arcata, California

Strain patterns within the forearc at a convergent margin adjacent to a passing fault-fault-trench triple junction show a systematic evolution. We describe late Neogene and Quaternary deformation in northern coastal California in the last 3 m.y. associated with the migration of the Mendocino triple junction. Deformation in the North American forearc near Humbolt Bay consists of a 30-km-wide zone of on-land contraction with a narrower zone of translation to the east. The zone of subaerial contraction is part of the relatively wide, southernmost extent of forearc contraction within the Cascadia subduction zone. Net Quaternary northeast-southwest contraction across forearc thrust faults is at least 7.9 km, and minimum fault slip rates on the six major thrust faults are 0.8–2.3 mm/yr. Net right slip within the zone of translation is a minimum of 3 km. South of the forearc, translation is predominant in the North American plate and is accommodated along two major right-lateral fault zones of the San Andreas transform boundary, the Lake Mountain, and Garberville fault zones. Discontinuous exposures of late Neogene sediments along these faults near Covelo and Garberville, respectively, indicate that crustal contraction, expressed by thrust faults and associated folding, predated translational deformation at each site. Inception of contraction near Covelo was related to inception of internal deformation of the Gorda plate at 3 Ma. This contraction, due to coupling of the convergent plates, migrated northward in the forearc in advance of and at the rate of migration of the triple junction. Present-day deformation near Humboldt Bay thus reflects contraction associated with subduction of the Gorda plate and translation farther east associated with oblique convergence at the plate boundary. As the triple junction migrates, the strike-slip faults of the San Andreas transform boundary will extend to the north-northwest into the present forearc, and forearc strike-slip faults will become faults of the San Andreas system. Contractional structures near Humboldt Bay will then cease to be active and will be preserved in the geologic record in the same way as contractional structures are preserved farther south.

INTRODUCTION

This paper has two purposes. The first is to describe late Neogene and Quaternary deformation in north coastal California in the past 3 m.y. The second is to relate the pattern of deformation preserved by the geology to plate interactions associated with the Mendocino triple junction. The Mendocino triple junction was the product of collision of the Pacific-Farallon ridge with the North American plate at about 28 Ma [*Atwater*, 1970]. The collision created two triple junctions that migrated away from each other as the San Andreas transform boundary extended in length. The Mendocino triple junction is at the northern end of this transform boundary (Figure 1).

Crustal deformation in north coastal California during the past 3 m.y. is in part the result of the geometric instability of the Mendocino triple junction as it migrates northward. If the fault-trench segment of the triple junction that bounds the North American plate does not describe a small circle, then the junction is unstable because it cannot retain its geometry as it moves [*McKenzie and Morgan*, 1969]. This type of instability creates extensional basins near the triple junction and landward jumps of the transform margin [*Dickinson and Snyder*, 1979*a*]. The Neogene structural basins of the northern California Coast Ranges provide evidence for the hypothesized extension that accompanies the northward propagation of the San Andreas transform margin [*Blake et al.*, 1978; *Dickinson and Snyder*, 1979*a*; *McLaughlin and Nilsen*, 1982]. Furthermore, a landward jump of the transform margin occurred about 10 Ma, when dominant right-lateral motion shifted from the San Gregorio-Hosgri fault system east to the San Andreas fault system [*Graham and Dickinson*, 1978].

Another source of triple junction instability is a change in relative plate motion [*Dickinson and Snyder*, 1979*a*]. Such a change occurred at the Mendocino triple junction, starting at about 2.5 Ma [*Silver*, 1971] or 3.0 Ma [*Wilson*, 1986], when Gorda-Pacific plate relative motion ceased to be parallel to the Mendocino fracture zone. This change in relative motion is recorded by bends in the magnetic anomalies on the southern Gorda plate [*Raff and Mason*, 1961]. Change in relative plate motion has been accommodated by deformation of the southern Gorda plate as it slides along the Mendocino fracture zone and is subducted under North America [*Silver*, 1971; *Jachens and Griscom*, 1983; *Wilson*, 1986].

The pattern of internal deformation of the Gorda plate, including rupture along northeast trending, left-lateral faults parallel to the trends of the bent magnetic anomalies, indicates north-south contraction [*Silver*, 1971; *McPherson et al.*, 1981; *Smith et al.*, 1981; *Wilson*, 1986]. Therefore, in the last 3 m.y., subduction of the internally contracting Gorda plate, rather than extension, is probably the major factor influencing crustal deformation on land near Cape Mendocino.

As a consequence of the northward elongation of the Pacific-North American transform boundary, there is no subducting slab beneath the North American plate south of the triple junction (called a slab window by *Dickinson and Snyder* [1979*b*]). In northern coastal California, deformation is more

Paper number 7B2052.
0148-0227/88/007B-2052$05.00

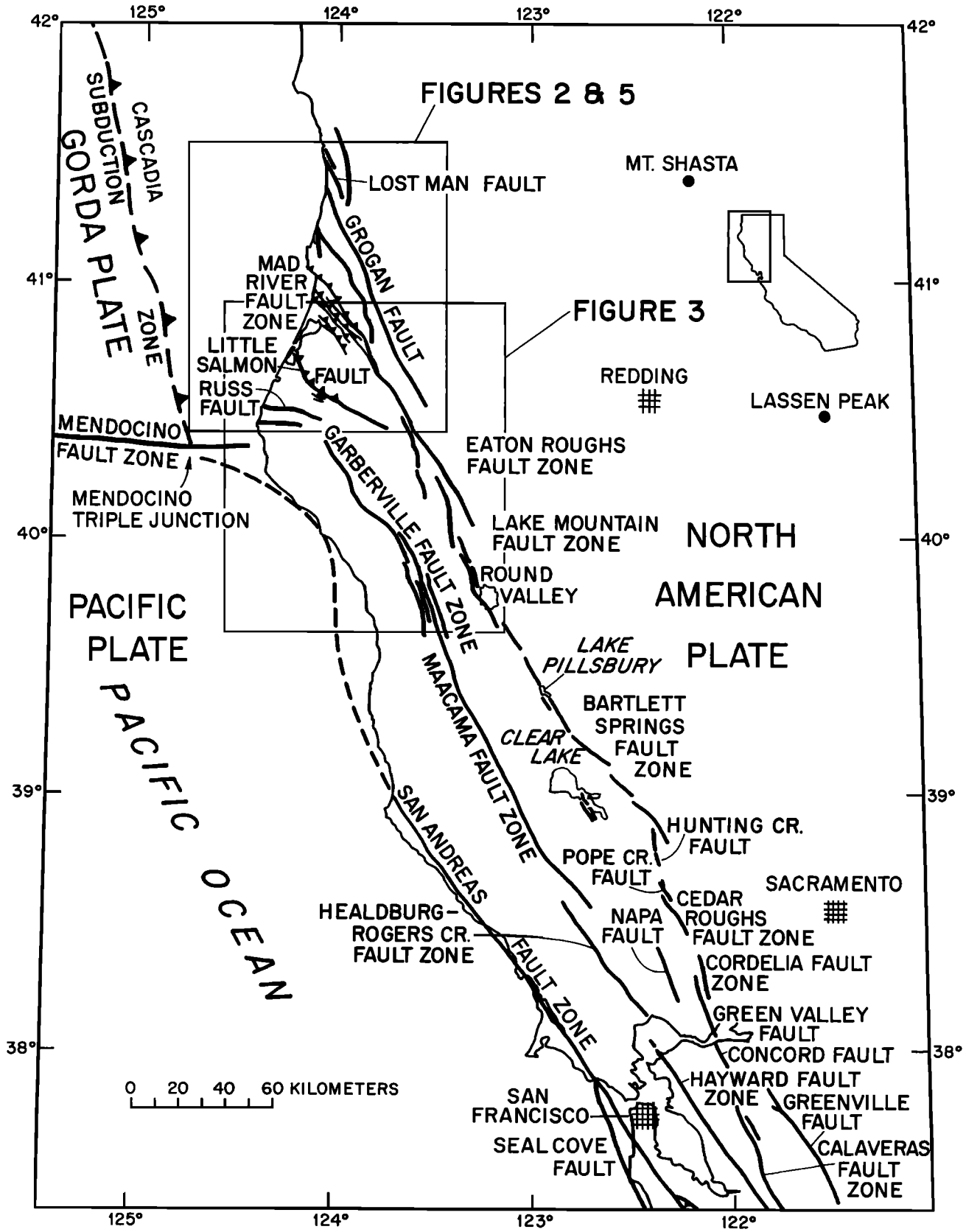

Fig. 1. Generalized tectonic map of northern California showing plate geometry and major faults. Modification of a compilation by *DePolo and Ohlin* [1984]. In addition to our mapping for the northern segment, sources include *Jennings* [1977], *Kelsey and Cashman* [1983], *McLaughlin* [1974], Steffen et al. (unpublished report, 1983), *Upp* [1982], *Wagner and Bortugno* [1982], and *Wright et al.* [1982].

complex and heterogeneous immediately north of the slab window. In this region, where the subducted Gorda plate underlies the accretionary margin of North America, crustal deformation includes components of both contraction and lateral translation. Farther south, above the slab window, deformation appears to be mainly by translational displacement on relatively straight, north-northwest trending strike-slip faults that occur as three distinct fault zones (Figure 1).

INVESTIGATIVE APPROACH

Mapping of Deformation

In order to document late Neogene and Quaternary crustal deformation in the study area (Figures 2 and 3), we selectively mapped areas of Quaternary and Neogene cover sediments. However, we did not do detailed field studies of the Neogene Wildcat Group sediments in the Eel River basin because previous studies [*Ogle*, 1953; *Woodward-Clyde Associates*, 1980] are available.

Late Neogene and Quaternary sediments cover about 20% of the area (Figures 2 and 3) and are concentrated near the coast. The Franciscan assemblage [*Blake and Jones*, 1981] forms the basement rocks. Where cover rocks are absent, post-Miocene deformation in the Franciscan could not be conclusively documented. However, on the basis of Quaternary landforms and fault offsets (detailed below) it is most probable that active faulting also occurs east of the area of Neogene cover.

We mapped by aerial photographic interpretation and field reconnaissance those fault zones that do not cut Neogene sediments but nonetheless appear to be active. We define a fault zone as a zone that comprises individual fault traces that are close together and share a similar trend. In order to map a fault zone as probably active, each fault within the zone had to meet the following criteria: (1) each fault must have a visually obvious trace defined by a prominent topographic lineament or trough hundreds of meters wide, (2) the trace must be accompanied by a linear trend of springs, indicating that the structure locally controls groundwater flow, (3) the trace must display at least two of the following features: aligned sag ponds, aligned notched ridges, aligned linear drainage segments, or ridgetop depressions, and (4) at least one of the traces within the fault zone must have offset a Neogene unit or a distinctive Franciscan melange block.

Faults shown by dashed lines on Figures 2 and 3 are major faults that cut Mesozoic basement rocks but do not meet the criteria for classification as probably active faults. Though sufficient geomorphic evidence is lacking, the dashed faults nonetheless may have been active in the Quaternary.

Mesoscale Structures

Associated with the major faults that cut Neogene and younger sediments is a broad (400–600 m wide) zone of fractures. These fractures can be divided into three classes: those with evidence of shear origin, called mesoscale (outcrop-scale) faults; those with evidence of extension origin, called extension fractures; and those of indeterminate origin, which we call fractures because they cannot be further classified.

Analysis of mesoscale faults was used as a field technique to differentiate megascale strike-slip faults from megascale reverse faults. This field technique has been further developed elsewhere [*Kelsey and Cashman*, 1983]. Somewhat related techniques, directed toward paleostress analysis, have been introduced by *Angelier* [1984] and utilized by *Angelier et al.* [1985], *Norris and Cooper* [1986], and *Frizzell and Zoback* [1987].

The type of strain recorded by mesoscale faults is apparent in outcrop by offset relations and slickenside striae or grooves on fault surfaces. Where fractures and faults occur together in groups of similar orientation (clusters), we assume the same origin for the fractures and the faults.

Mesoscale fractures and faults are ubiquitous in the late Neogene sediments of the study area. Generally, these structures increase in density within 200–300 m either side of megascale faults, with greatest density near the fault trace. We therefore consider mesoscale faults as genetically related to the megascale fault.

Pairs of fault sets are common at many measuring sites. The sets are separated by an acute angle. In cases where the two fault sets formed synchronously (each offsets the other), have opposite senses of displacement, and show displacement perpendicular to the line of intersection of the fault sets, the two fault sets are a conjugate fault pair [*Hobbs et al.*, 1976].

We found two types of conjugate faults in Neogene sediments near megascale faults. In type one, all faults were vertical or subvertical, and all indicators of fault slip were horizontal or subhorizontal. In type two, all faults dipped less than 60°, all indicators of fault slip showed a downdip sense, and offsets showed a reverse movement sense.

Conjugate strike-slip shears are associated wih transcurrent fault systems [*Harding*, 1973; *Wilcox et al.*, 1973]. However, the orientation of conjugate shears does not provide an unequivocal direction for the principal strain axes, despite models [*Wilcox et al.*, 1973] that show such a relation under idealized conditions. Orientation of the strike-slip conjugate faults relative to the principal strain for the region varies depending on postfaulting tectonic rotation and on where the conjugate fault developed along a segmented fault zone [*Sibson*, 1986]. Therefore conjugate strike-slip faults are used to document megascale transcurrent fault deformation, but we will not use these faults to assess axes of principal strain.

In the portion of the study area north of the latitude of the Little Salmon fault (Figure 2), the cover sediments are Pliocene and Pleistocene, and only one deformation is present. In this area we could establish a correlation of low-angle conjugate faulting (at the mesoscale) with thrust faults (at the megascale). Similarly, high-angle conjugate mesoscale faults are associated with high-angle, dominantly strike-slip megascale faults.

In the study area near the Russ fault and farther southward (Figure 3) the Neogene sediments appear to have two generations of deformation, based on offsetting relations of the megascale faults. Regional folding is associated with the first deformation.

Classification of Crustal Strain

Crustal strain is dominated either by contraction (thrust faults, reverse faults, folds) or lateral translation (high-angle faults that in all cases have strike-slip displacements that are much greater than any observed dip-slip displacements). Crustal extension is not a regionally significant type of strain in northern coastal California. However, many outcrops show extension, and extensional strain is significant at fault bends and stepovers in the strike-slip fault zones. Intermontane valleys in the coast ranges (Figures 2 and 3) are geomorphic expressions of such localized extension.

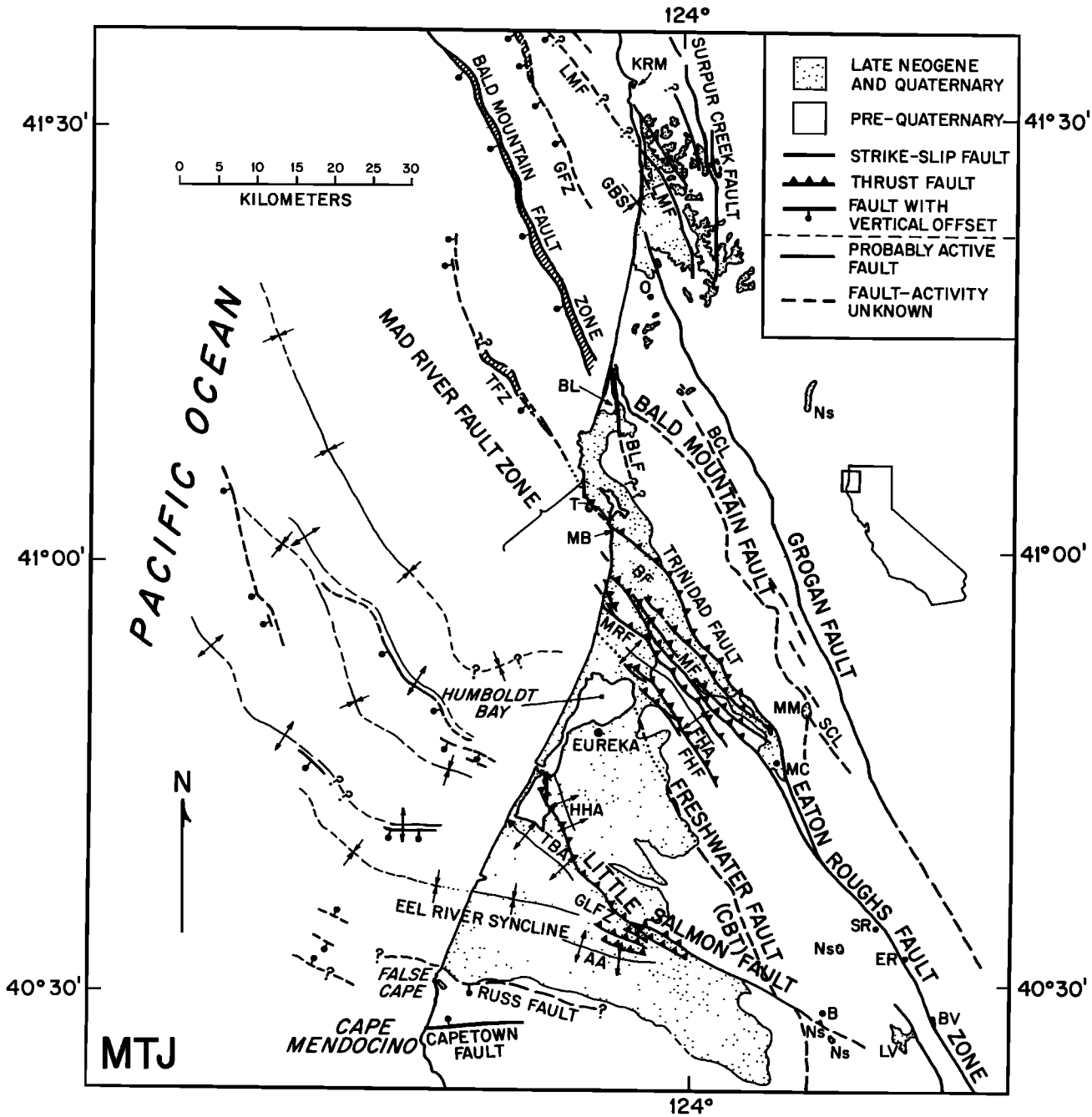

Fig. 2. Tectonic map of north coastal California north of Cape Mendocino. Offshore data from *Clarke* [1987]. Faults with solid lines are probably active (for criteria, see text); faults with dashed lines do not meet criteria of probably active faults. Faults: LMF, Lost Man fault; GFZ, Grogan fault zone (offshore only); BCL, Bridge Creek lineament; BLF, Big Lagoon fault; Trinidad fault zone (offshore only); BF, Blue Lake fault; MF, McKinleyville fault; MRF, Mad River fault; FHF, Fickle Hill fault; SCL, Snow camp lineament; CBT, coastal belt thrust. Folds: Gold Bluffs syncline; FHA, Fickle Hill anticline; HHA, Humboldt Hill anticline; TBA, Table Bluff anticline; AA, Alton anticline; RS, Redway syncline. Intermontane valleys: MM, Murphy's Meadows; LV, Larrabee Valley; BV, Burr Valley. Water bodies: AB, Arcata Bay; HB, Humboldt Bay. Localities: O, Orick; T, Trinidad; MB, Moonstone Beach; A, Arcata; E, Eureka; B, Bridgeville; D, Dinsmore. Geologic units: dot pattern, all late Neogene and Quaternary sediments (mid-Miocene to present; excludes Miocene rocks of Kings Range terrane of *McLaughlin et al.* [1982]); no pattern, early Cenozoic and pre-Cenozoic rocks of Franciscan assemblage (includes Kings Range terrane) and Klamath Mountain province; NS, isolated patches of late Neogene sediments, age designation uncertain; MTJ, approximate location of Mendocino triple junction.

CONTRACTIONAL DEFORMATION

Late Neogene and Quaternary sediments record crustal contraction in the Humboldt Bay area of north coastal California. Contemporaneous deformation is occurring along the Mad River fault zone and in the lower Eel River valley (Figure 2). Crustal contraction, probably active in the latter part of the Neogene but probably not active today, is documented near Garberville and near Covelo, California.

Mad River Fault Zone

The Mad River fault zone [*Carver et al.*, 1983] is a set of northwest trending, northeast dipping imbricate thrust faults

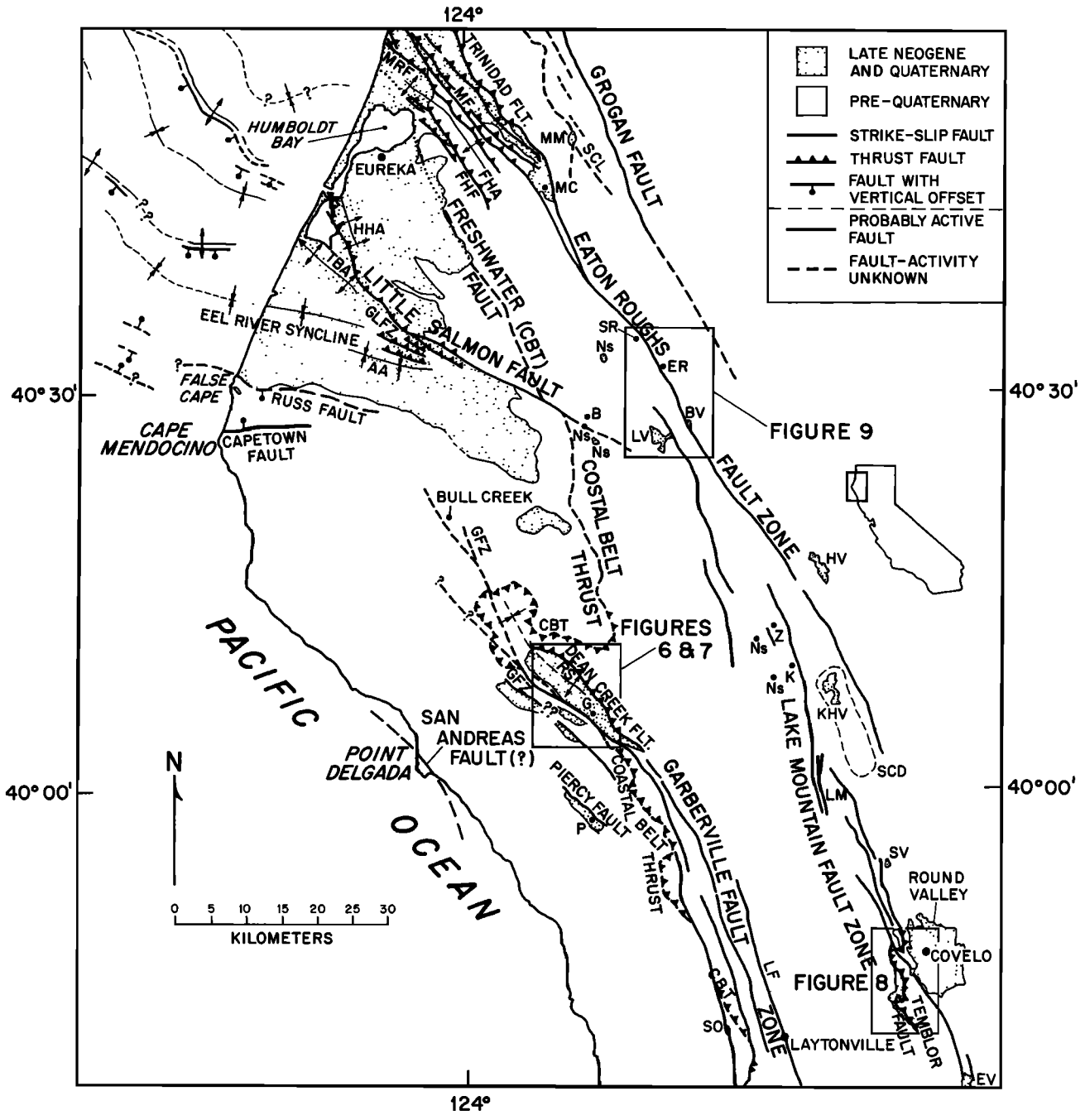

Fig. 3. Tectonic map of northern terminus of San Andreas fault zone. Offshore data from *Clarke* [1987]. See caption to Figure 2 for abbreviations and explanations that are not noted below. Faults: CBT, coastal belt thrust; GFZ, Garberville fault zone; DCF, Dean Creek fault; LF, Laytonville fault; TF, Temblor fault. Folds: FHA, Fickle Hill anticline; HHA, Humboldt Hill anticline; TBA, Table Bluff anticline; AA, Alton anticline; RS, Redway syncline. Intermontane valleys: HV, Hettenshaw Valley; KHV, Kettenpom-Hoaglin valleys; SCD, Salt Creek depression; SV, Summit Valley; RV, Round Valley; SO, Stoten opening; EV, Eden Valley. Localities: G, Garberville; Z, Zenia; K, Kettenpom; LM, Lake Mountain; P, Piercy; C, Covelo.

that extend from the coast approximately 40 km inland to the vicinity of Maple Creek (Figures 2 and 5). The fault zone contains five principal thrust faults (Trinidad, Blue Lake, McKinleyville, Mad River, and Fickle Hill faults) and numerous minor thrust faults. Road cut exposures and exploratory trenches [*Woodward-Clyde Associates*, 1980] show that the faults dip between 20° and 40° (Table 1). The Blue Lake anticline and Fickle Hill anticline constitute major folds within the zone (Figure 2). The folds are asymmetrical, with northern anticlinal limbs dipping 20°–30° and southern limbs nearly vertical and locally overturned. Fold axes parallel the trend of the thrusts (N35°–40°W) and plunge gently north-northwest. Fold limbs are cut by the thrust faults. The faults offset the Pleistocene marine and fluvial sediments of the Falor Formation (age of the Falor Formation is discussed below) [*Manning and Ogle*, 1950] and offset late Pleistocene fluvial and marine terraces near the coast [*Carver et al.*, 1986].

Net dip slip on each of the faults can be estimated by the

TABLE 1. Summary of Fault Deformation in the Mad River Fault Zone Based on Displacements of the Falor Formation Basal Contract

Fault or Fault Zone	Location	Age,[a] Ma	Dip	Vertical Displacement, m	Dip-Slip Displacement, m	Slip Rate, mm/yr
Trinidad fault	Canon Creek	0.7	40°	575	900	1.3
Blue Lake fault	Canon Creek	0.7	40°	750	1200	1.6
Blue Lake fault	Korbel	0.7	35°	950	1600	2.3
McKinleyville fault	Simpson Timber Company Road 4500	0.7	35°	300	525	0.8
Mad River fault	Simpson Timber Company Road 5400	0.7	35°	325	575	0.8
Fickle Hill fault	Jacoby Creek	0.7	25°	350	825	1.2
Mad River fault zone	Jacoby Creek-Korbel Section	0.7	35°	2500	4400	6.4

[a]Age is the age of initiation of faulting assuming faulting commenced with termination of Falor deposition, or a little more than a million years after eruption of the Huckleberry Ridge tuff. See discussion in text.

amount of offset of the basal depositional contact of the Falor Formation on the Franciscan assemblage. Net dip slip for each fault ranges from 525 to 1600 m (Table 1). Using the range of dip and the amount of dip-slip displacement for the five thrust zones, net horizontal shortening across the Mad River fault zone in Pleistocene time due to low-angle faulting must be about 3.6 km along a northeast-southwest axis.

A minimum shortening rate for the Mad River fault zone (assuming that all shortening is due to low-angle faulting) is provided by a maximum age for the Falor Formation. This maximum age comes from a volcanic ash near the depositional base of the Falor, which is correlated by its geochemistry to the 1.8–2.0 Ma Huckleberry Ridge tuff from the Yellowstone caldera [*Sarna-Wojcicki et al.*, 1987]. Minimum horizontal shortening rate across the Mad River fault zone since 1.8–2.0 Ma is therefore approximately 1.8–2.0 mm/yr.

In all measured stratigraphic sections the top of the Falor Formation has been removed by faulting, but the minimum thickness is in excess of 940 m. The formation includes poorly consolidated interbedded clays, silts, sands, pebbly sands, and gravels deposited in conditions ranging from shallow open marine to beach, estuarine, and fluvial environments. The lack of angular unconformities with significant stratigraphic relief indicates that Mad River fault zone faulting and folding were not active during deposition of the Falor sediments. Therefore we feel that it is likely that Mad River fault zone deformation did not accompany Falor deposition but rather it was the development of fault and fold structures that terminated Falor deposition.

Time span of Falor deposition is not well constrained at the younger limit. Deposits at Moonstone Beach south of Trinidad (MB, Figure 2), which are either upper Falor Formation or a younger overlying unit (W. Miller III, personal communication, October 1986), yield age estimates of somewhere between 0.35 and 1.0 Ma based on measured $^{230}Th/^{234}U$ and $^{234}Th/^{238}U$ ratios on the coral *Balanophyllia elegans* (B. Szabo, written communication to W. Miller III, April 1985). These ages for the youngest Falor sediments suggest a depositional interval for the Falor Formation of about 0.9–1.5 Ma (assuming that deposition commenced at about the time of the volcanic ash).

From the above estimates, tectonic activity in the Mad River fault zone was initiated about 0.9–1.5 m.y. after deposition of the volcanic ash, or 0.4–1.0 m.y. before present. Averaging this time interval, we assume that tectonic activity commenced about 0.7 Ma.

If horizontal shortening spanned the last 0.7 m.y., then the actual shortening rate is at least twice that calculated from the maximum age of the Falor sediments. In Table 1 we assume that faulting commenced at 0.7 Ma, or approximately 1.2 m.y. after deposition of the Huckleberry Ridge ash. Given this age for fault initiation, dip-slip displacement of the basal Falor contact on individual faults in the Mad River fault zone yields fault dip-slip rates ranging between 0.8 and 2.3 mm/yr (Table 1). Summing these slip rates across the fault zone yields a net slip rate of 6.4 mm/yr, or (assuming an average thrust fault dip of 35°) 5.2 mm/yr of NE-SW horizontal shortening during the last 0.7 m.y. This net 3.6 km of NE-SW horizontal shortening from documented thrust faults is a minimum estimate. Additional contraction of unknown magnitude must exist due to folding associated with the mapped thrust faults as well as faulting on other unidentified Neogene contractional structures that likely occur in Franciscan rocks to the northeast.

Deformation of the late Pleistocene marine terraces provides an independent measure of shortening rate across the Mad River fault zone [*Carver et al.*, 1986]. From one to seven raised marine terraces straddle the Trinidad, McKinleyville, Mad River, and Fickle Hill faults. The older terraces are progressively offset by greater amounts (Figure 4). *Burke et al.* [1986] assigned ages to the terraces (Figure 4) by correlation of the altitude distribution of the terraces on the upfaulted (northeastern) fault blocks to worldwide high sea level stands defined by dated marine terraces at New Guinea [*Bloom et al.*, 1974; *Chappell*, 1983]. Terrace age assignments are according to methods and assumptions discussed by *Bull* [1985]. From the terrace displacement and age data, dip-slip displacement rates for the four faults of the Mad River fault zone in the last 0.2 m.y. are 0.9, 0.9, 1.2, and 0.8 mm/yr, respectively (Figure 4). Cumulative dip-slip displacement rate during the late Pleistocene is therefore about 3.8 mm/yr. This minimum rate (which excludes the Blue Lake fault (BL, Figure 2) that does not cut Pleistocene surfaces) is equivalent to a horizontal shortening of about 3.3 mm/yr, which is somewhat less than the minimum shortening rate of 5.2 mm/yr based on offset of Falor-Franciscan contacts.

Thrust faults of the Mad River fault zone are active. Not only do these faults offset late Pleistocene marine terraces with scarps of 15–90 m, but one of the faults offsets a Holocene fluvial strath terrace in the lower Mad River valley by 7 m.

Mesoscopic faults increase in intensity toward the thrust faults of the Mad River fault zone. These faults, measured within 200 m of the individual major thrust faults, are low angle and form a conjugate set (Figure 5, sites A and B). Where bedding in the Falor Formation is horizontal, the con-

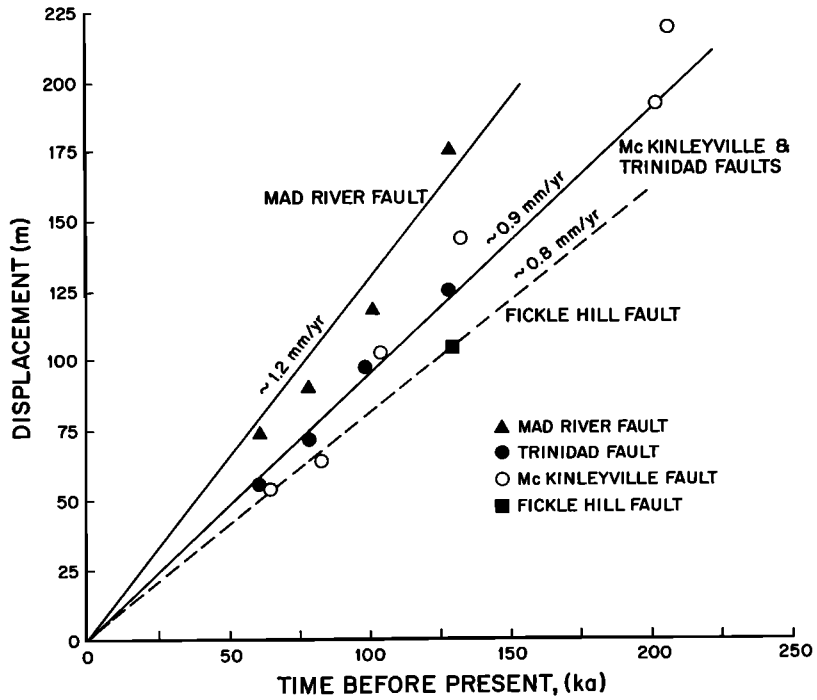

Fig. 4. Dip-slip displacement magnitudes for faults of the Mad River fault zone (y axis) plotted against terrace ages (x axis). Dip-slip displacement calculated from vertical terrace offset and an assumed fault dip of 25°. Dip-slip estimates for the Fickle Hill and Mad River faults are minimum estimates because the downfaulted side of the terrace is buried beneath Holocene alluvial deposits. Terrace age determinations discussed in text.

jugate set is symmetric about a vertical plane (Figure 5, site B). Where Falor Formation bedding is inclined, conjugate symmetry of faults about a vertical plane is restored by rotation of these features with bedding as bedding is rotated back to horizontal (Figure 5, site B unrotated versus B rotated). At site B, not only is conjugate symmetry restored by rotation, but the mean fault pole directions for the fault pole clusters are both defined with a smaller α_{95} confidence limit [*Fisher*, 1953] after rotation (Table 2).

From the structural data we infer that these mesoscale low-angle reverse faults formed prior to folding related to movement on the major fault. The mesoscale faults formed only during incipient movement on the master fault, at a time when strain was more evenly distributed across the 500- to 1000-m-wide fault zone and before strain was concentrated on the master faults of Figure 5.

Lower Eel River Valley and Humboldt Bay Area

The lower Eel River valley and the adjoining Humboldt Bay area show abundant evidence of northeast-southwest contraction. The late Tertiary and Quaternary Wildcat Group [*Ogle*, 1953; *Woodward-Clyde Associates*, 1980] is deformed in a series of west-northwest to northwest trending folds. Most notable of these is the Eel River syncline (Figure 2), which has been a site of deposition since at least mid-Miocene [*Ogle*, 1953]. Other folds include the Alton anticline, Table Bluff anticline, and Humboldt Hill anticline (Figure 2) [*Ogle*, 1953]. Late Pleistocene marine and fluvial terraces are cut on the flanks and noses of all these folds, and these surfaces dip in a fashion sympathetic to, but less steeply than, the Wildcat sediments, suggesting the folds have been growing throughout the Pleistocene. Low-angle reverse and thrust faults cut the flanks of these folds [*Woodward-Clyde Associates*, 1980] (Figure 2). These folds probably originated above faults that did not originally rupture to the surface, and the folds propagated as the fault grew stratigraphically upward [*Suppe*, 1985]. The proximity of the Humboldt Hill anticline to the northwest end of the Little Salmon fault provides an example of a likely fold-thrust fault pair.

The Little Salmon fault is the major thrust fault of the southern Humboldt Bay area [*Ogle*, 1953] (Figure 2). The character of this fault has been investigated by *Woodward-Clyde Associates* [1980]. The dip of the Little Salmon fault ranges from 20° to 30°. Progressively smaller amounts of displacement on successively younger beds indicate that the Little Salmon fault has undergone repeated displacement since the late Pleistocene. Total cumulative vertical displacement near Humboldt Bay is approximately 2 km, which implies that net northeast-southwest directed contraction due to thrusting just on the Little Salmon fault is at least 4.3 km. Correlation of dated horizons from drill hole borings through the hanging wall and footwall of the fault indicates a minimum slip rate for the fault in the last 0.8 m.y. of 1.3 mm/yr. Correlation of other horizons yields slip rates as high as 2.2 mm/yr. Other faults associated with the Little Salmon fault are the Goose Lake fault (Figure 2) and the Bay Entrance fault [*Woodward-Clyde Associates*, 1980]. In a general sense, the Little Salmon fault and associated structures have accommodated northeast-southwest directed contraction in the same manner as faults and folds of the Mad River fault zone farther to the north, though the direction of maximum shortening has a slightly more northerly orientation.

Contraction in the Eel River valley–Humboldt Bay area appears to be active, based on warping of late Pleistocene surfaces. The last movement on the Goose Lake fault zone was less than 6300 years B.P. [*Woodward-Clyde Consultants*,

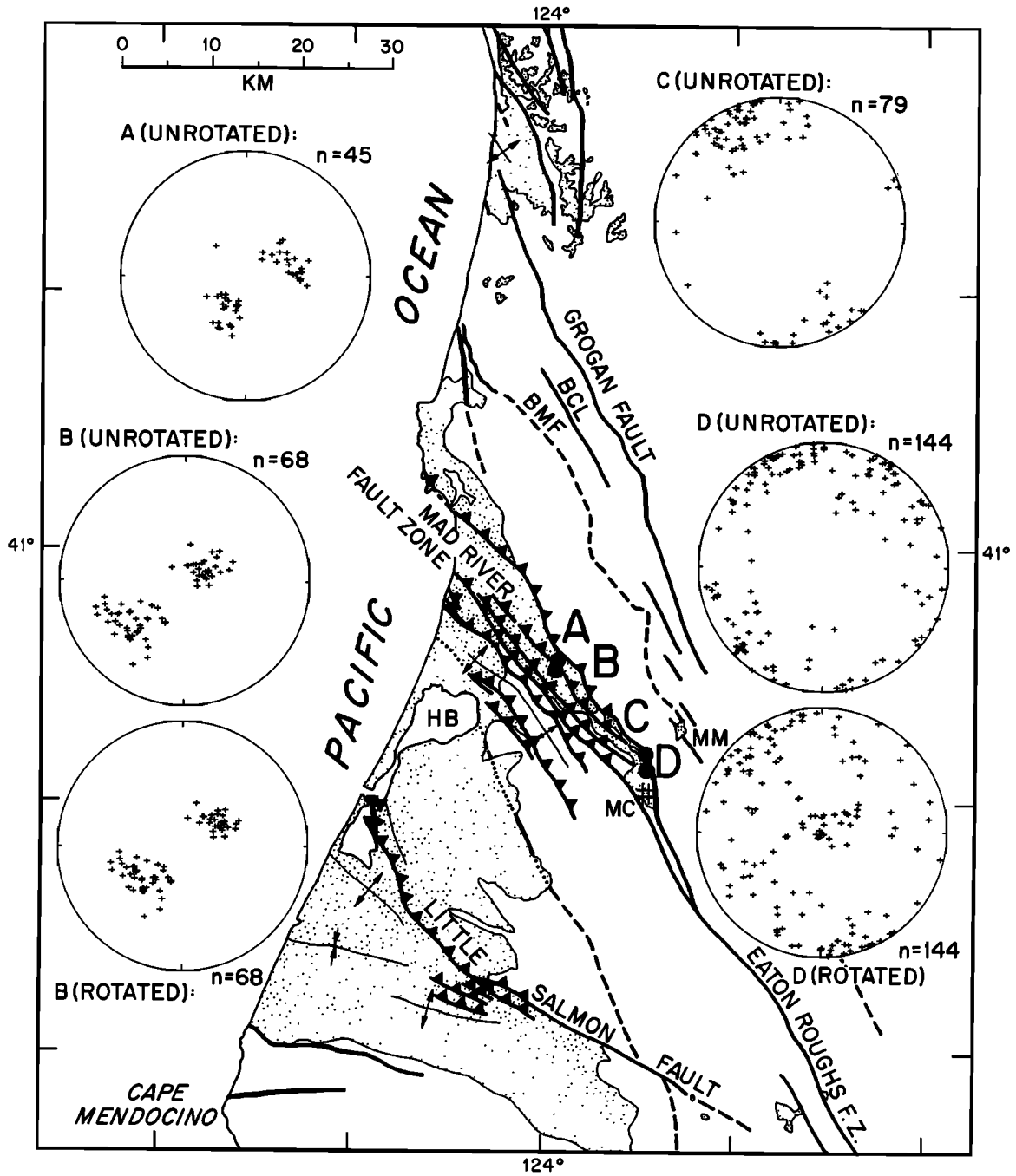

Fig. 5. Map of the Mad River fault zone and the northern terminus of the Eaton Roughs fault zone showing pole-to-plane lower hemisphere spherical projections of mesoscale fracture and fault plane data. Unrotated data are raw data from the outcrop. Rotated data are rotated with bedding as bedding is rotated to horizontal. Original bedding was horizontal at sites A and C. See further discussion in text. BCL, Bridge Creek lineament; BMF, Bald Mountain fault; HB, Humboldt Bay; MC Maple Creek; MM, Murphy's Meadows.

1980], on the basis of a ^{14}C date on charcoal in faulted lake deposits. Trenches excavated across the Little Salmon fault show folded and faulted valley fill sediments of Holocene age.

Garberville Sediments and Dean Creek Fault

The basic structural geology of the Garberville sediments (Figure 6) was first recognized by *MacGinitie* [1943]. In a more thorough study, *Menack et al.* [1985] and *Menack* [1986] divided these sediments into two informally named units, the Kimtu unit (the two southwestern outcrop belts) and the Garberville unit (northeastern outcrop belt) (Figure 6). Biostratigraphic studies (diatoms and mollusks) by *Menack* [1986] indicate that the Kimtu is older than the Garberville (late early to middle Miocene versus late Miocene to Pliocene, respectively), but the upper ages of both units are unconstrained due to erosion. Our mapping indicates that structurally the two units are difficult to distinguish. Each outcrop belt is in depositional contact on top of the Franciscan to the southwest and in fault contact with the Franciscan to the northeast (Figure 6). Each belt has a regional strike to the

TABLE 2. The α_{95} Confidence Limits for Fisher Means of Clusters of Poles to Mesoscale Faults: Figure 5, Site A: Unrotated Fault Data Versus Rotated Fault Data

Pole Cluster	α_{95} Confidence Limit for Unrotated Cluster	α_{95} Confidence Limit for Rotated Cluster
SW quadrant	3.9°	3.3°
NE quadrant	4.4°	3.9°

northwest and dips moderately to the northeast. Beds are locally folded and overturned near the northeast fault contact in each unit. We presume that this folding and local overturning are due to movement on the northeast bounding faults (Figure 6).

None of the three northeast bounding faults are exposed, and fault dip is uncertain from direct observation. One of these faults, the Dean Creek fault, truncates the Garberville unit (Figure 6). Mesoscale structures increase in density toward the Dean Creek fault both along the South Fork Eel River and the Alderpoint Road. Pole-to-plane spherical projections of mesoscale faults at these sites (sites A and B, Figure 7) show distinct clusters of poles. These fault poles form two moderate to low-angle conjugate pairs, symmetric about a vertical plane, only after the faults are rotated with bedding as bedding is rotated to horizontal.

The pattern of mesoscale faults adjacent to the Dean Creek fault is similar to the fault pattern in the Mad River fault zone. The conjugate pattern at Garberville is more diffuse due to an apparent second generation of faulting along the Garberville fault zone (discussed below). Despite the added complexity, a pattern of low-angle faulting is associated with the Dean Creek fault, and we infer that the Dean Creek fault is a thrust or low-angle reverse fault that places Franciscan melange over Garberville sediments. As in the Falor Formation, the mesoscale low-angle faults probably formed during initial contractional deformation before the Dean Creek fault had substantial displacement. Though the other two faults that cut the two outcrop belts of the Kimtu unit are probably the same age and same structural style, they are poorly exposed. Stream bank exposures of the fault cutting the southwesternmost Kimtu unit (Figure 6) suggest that it is a low-angle reverse fault.

Temblor Formation and Temblor Fault

The Miocene Temblor Formation of *Clark* [1940], exposed near Covelo, California (Figure 8), is a sequence of fluvial gravels, sands, and coal, interbedded with clayey, silty sands of estuarine and marine origin. The formation is largely obscured by vegetation and landsliding; exposures of fine-grained sediment are rare, and mesoscopic fault and fractures are seldom observed.

The structural setting of the Temblor Formation is similar to that of the Garberville sediments. The formation strikes predominantly north-northwest, is deposited on the Franciscan to the southwest, and is in fault contact with the Franciscan to the northeast along the Temblor fault. We infer the fault contact to be low angle because (1) the outcrop pattern of the fault is highly sinuous and topographically conforms to an irregular, low-angle fault plane, (2) in summit areas of low relief (where landslide deposits could not accumulate unless there was a topographic inversion during erosion), dense crystalline blocks from the Franciscan melange appear "deposited" in a matrix of Temblor debris, a situation that can most reasonably be explained if an overlying Franciscan unit erosionally downwasted (through a low-angle fault) into a lower horizon of Temblor sediment, and (3) two three-point solutions on the faulted Temblor contact taken across stream valleys indicate fault dips of 6° and 18°. The amount of dip slip on the fault is unknown. The main body of Temblor sediments pinches out to the north, possibly because the entire thickness of exposed sediments (elsewhere at least 400 m thick) has been thrust under the Franciscan melange along the Temblor fault. The Temblor fault postdates deposition of the Temblor Formation, but its timing cannot be further constrained.

TRANSLATIONAL DEFORMATION

North of the latitude of the Mendocino triple junction, translational deformation occurs along a narrow zone within the forearc, both to the east and the north of the zone of contraction. South of the approximate latitude of the triple junction, the San Andreas fault system consists of a broad, 65- to 80-km-wide belt of translational deformation.

Grogan–Lost Man Fault Zone

North of Big Lagoon, the Pliocene and Pleistocene (predominantly Pleistocene) Prairie Creek Formation [*Kelsey and Cashman*, 1983; *Cashman et al.*, 1988] (top of Figure 2) outcrops in a 125 km^2 coastal area. The sediments are the onshore part of an extensive sequence of sediments deposited on the continental shelf at the mouth of the Klamath River. A prominent structure in the unit is the northwest trending, slightly northwest plunging Gold Bluffs syncline (GBS, Figure 2). The northeast limb of the syncline is steeper and cut off by faulting.

Three major megascale faults, as well as a number of minor megascale faults, offset the Prairie Creek Formation (Figure 2). Two of these faults, the Grogan fault and the Sulphur Creek fault, are each exposed in a single exposure, and the Lost Man fault is not exposed at all. However, abundant mesoscale faults and fractures occur in Prairie Creek sediment in proximity to the Lost Man fault and to a lesser extent near the Grogan fault. These features are predominantly high angle and form conjugate sets [*Kelsey and Cashman*, 1983]. Analysis of these faults and fractures in conjunction with mesoscale, deformation-related normal faults, thrust faults, and folds led *Kelsey and Cashman* [1983] to infer that the Lost Man and Grogan faults were right-lateral high-angle faults that have an appreciable, but less significant, component of reverse dip-slip offset as well. Because of extensive erosion, sense of fault offset cannot be inferred from outcrop distribution alone. However, the outcrop distribution of Prairie Creek sediments in relation to the two faults constrains right-lateral offset to less than 10 km.

In addition to being associated with high-angle mesoscale structures the Grogan and Lost Man faults have linear fault traces over rugged topography. These characteristics are in contrast to the imbricate thrust faults of the Mad River fault zone that have irregular traces over equally rugged topography and are associated with low-angle, mesoscopic faults and fractures. The thrust faults of the Mad River fault zone trend N35°–40°W, whereas the Grogan and Lost Man faults trend N25°W and N10°–15°W, respectively.

Though we interpret both the Grogan and Lost Man faults as predominantly high-angle strike-slip faults, a reverse slip component is present as well. The Grogan fault in the one locality where it is exposed shows a sharp fault contact with

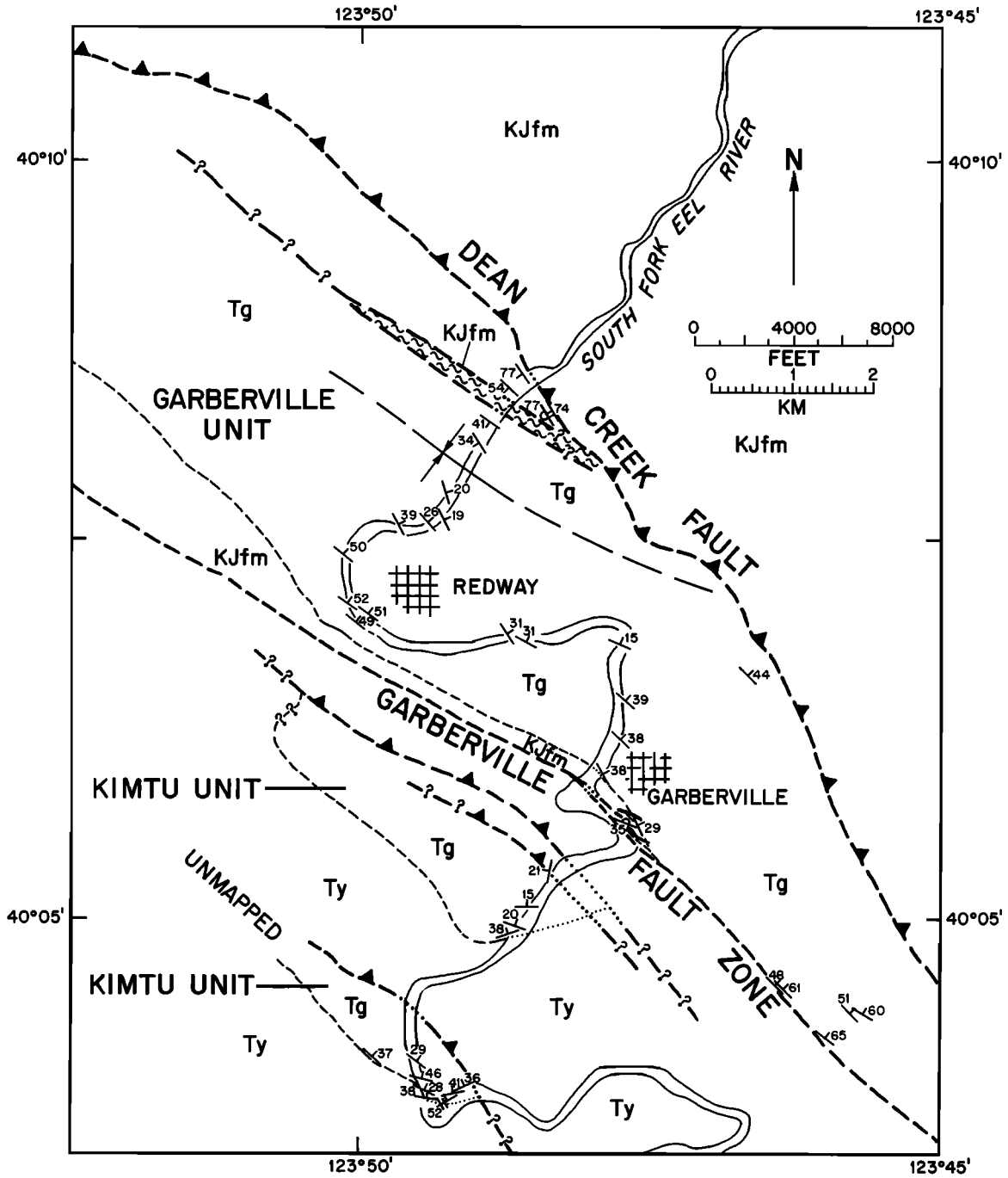

Fig. 6. Geologic structure map of the Neogene Garberville sediments (Tg), in the vicinity of Garberville, California. The map is designed to show outcrop extent and structure in unit Tg, the pre-Cenozoic geology is highly generalized. The Ty/KJfm contact is taken in part from R. J. McLaughlin et al. (manuscript in preparation, 1988), 1 : 100,000 Garberville 1° sheet geologic map. Ty, Franciscan Yager sediments (Paleogene); KJfm, Franciscan melange.

an attitude of N28°W, 54°NE, and small fractures in sands beneath the fault are mostly low angle. Regionally (within 1 km of the fault), however, mesoscopic structures associated with the Grogan fault are high angle [*Kelsey and Cashman*, 1983]. There is therefore the possibility that dip-slip motion may be as important as strike-slip motion for the Grogan fault where it cuts Prairie Creek sediments.

Both the Grogan and Lost Man faults are major fault zones that appear to be reactivated Mesozoic tectonic features. The Grogan, in particular, has accommodated upward of 75 km of right slip in the Tertiary [*Kelsey and Hagans*, 1982; *Blake et al.*, 1985].

South of Orick, California (O, Figure 2), Quaternary translational motion on the Grogan and Lost Man faults cannot be demonstrated because Pliocene or Pleistocene cover sediments are absent. The south-southeastern extent of the Grogan fault as a possibly active Quaternary structure is unknown. The tectonic map (Figure 2) shows that the Eaton Roughs–Lake Mountain fault zone is the easternmost active Quaternary structure south of latitude 40°30'N. It is possible, however,

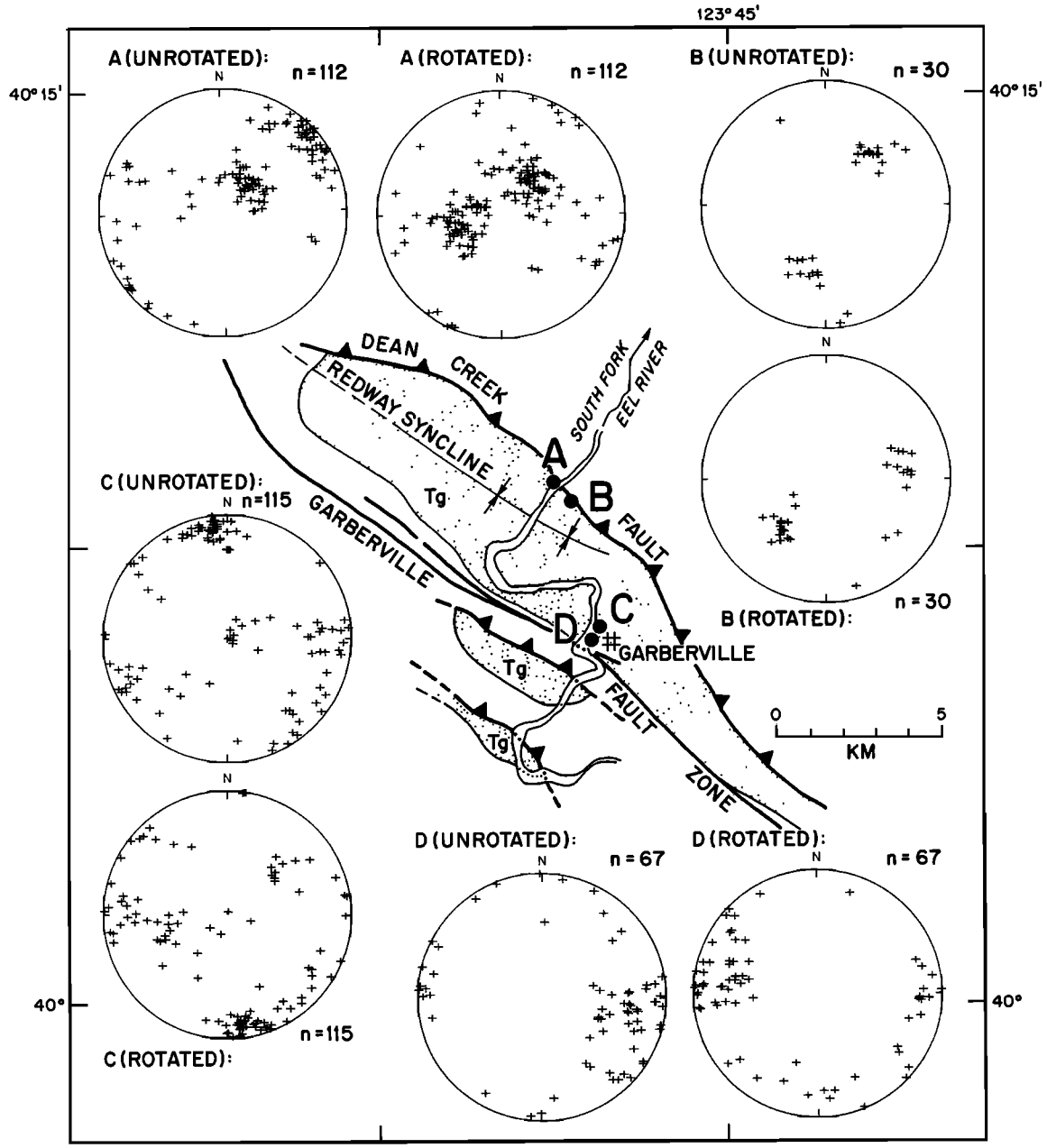

Fig. 7. Pole-to-plane lower hemisphere spherical projections of mesoscale fracture and fault plane data for sites along the faulted margins of the Garberville sediments (Tg). Unrotated data are raw data from the outcrop. Rotated data are rotated with bedding as bedding is rotated to horizontal. See discussion in text.

that the southern part of the Grogan fault, or related faults, has accommodated dextral translational strain in the Quaternary.

Eaton Roughs Fault Zone

The Eaton Roughs fault zone is defined by numerous undrained depressions, linear drainage segments, and instances of unstable ground that together define a north-northwest trending straight trace for 66 km from Maple Creek southsoutheast to its merger with the Lake Mountain fault zone [*Kelsey and Allwardt*, 1983] (Figure 2). The fault zone is named after Eaton Roughs, a distinctive tabular body of resistant Mesozoic graywacke sandstone north of Dinsmore, California, which is offset right laterally 3.3 km from an identical isolated tabular graywacke body, Showers Rock. The trace of the Eaton Roughs fault zone separates these bodies (Figure 9).

The northern 12 km of the Eaton Roughs fault zone consist of two straight traces that trend north-northwest into the most landward (easterly) exposures of the Falor Formation (Figures 2 and 3). The Falor sediments are vertically offset (and perhaps laterally offset as well) by at least one trace of the Eaton Roughs fault, demonstrating that there has been movement on the fault since 0.4–1.0 Ma.

We investigated deformation at the transition of the Mad River fault zone and the Eaton Roughs fault zone by analyzing the mesoscale faults in the easternmost Falor sediments near Maple Creek compared to those in the western Falor

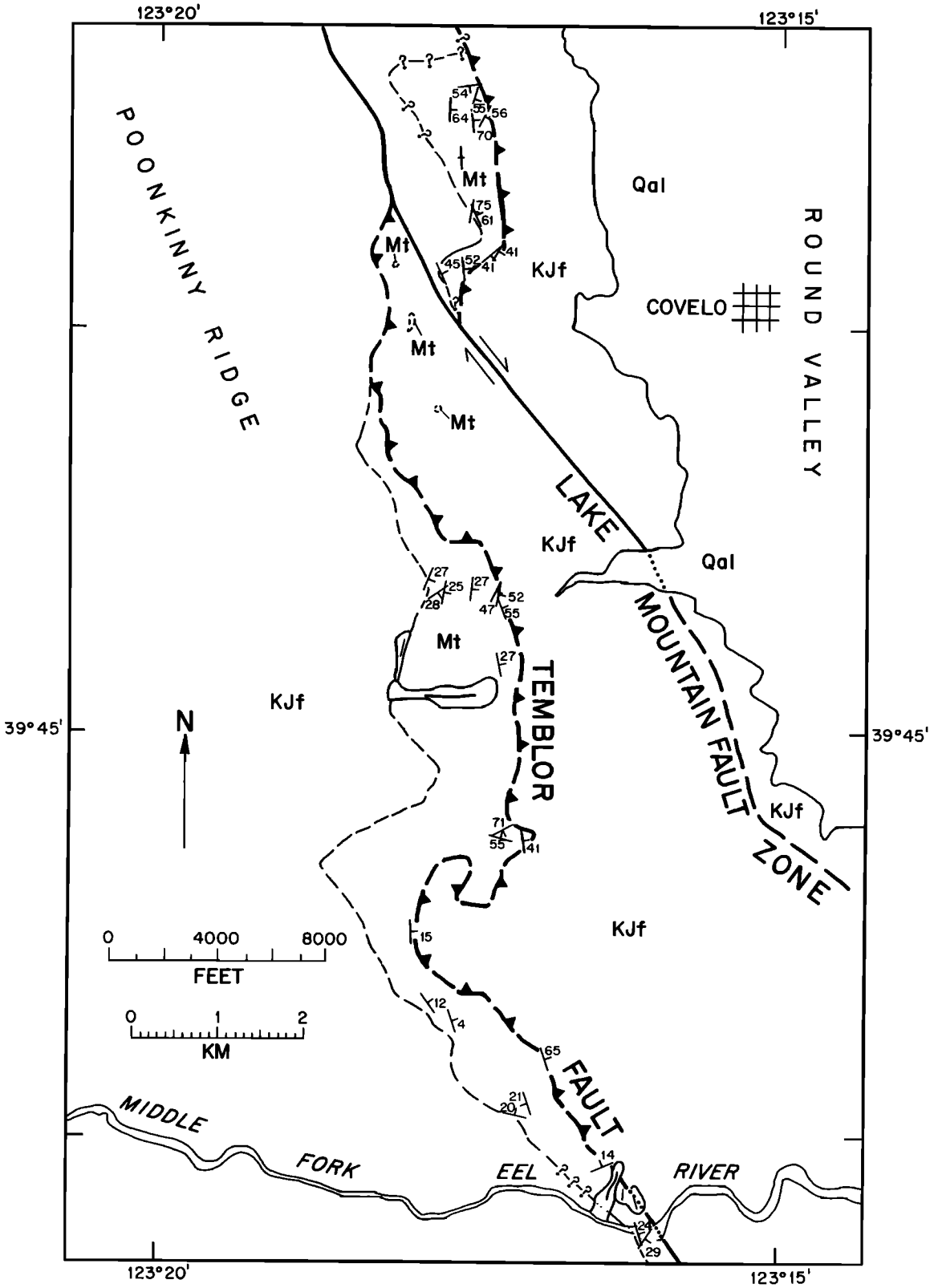

Fig. 8 Geologic map of the Miocene Temblor Formation (Mt) near Covelo, California. The map shows outcrop extent and structure in unit Mt; the pre-Cenozoic geology is highly generalized (KJf, Franciscan assemblage). Also shown are two traces of the Lake Mountain fault zone. One of these traces right laterally offsets unit Mt and the Temblor fault.

sediments near the coast. As already discussed, the Falor sediments near the coast are offset by megascale, imbricate thrust faults and mesoscale low-angle faults (Figures 2 and 3). Mesoscale faults and fractures in the eastern Falor sediments (sites C and D, Figure 5) are mainly high angle, and restoration of these sediments to horizontal bedding does not restore the faults and fractures to a low-angle, conjugate pattern (site D, Figure 5). To the contrary, restoration of these features to

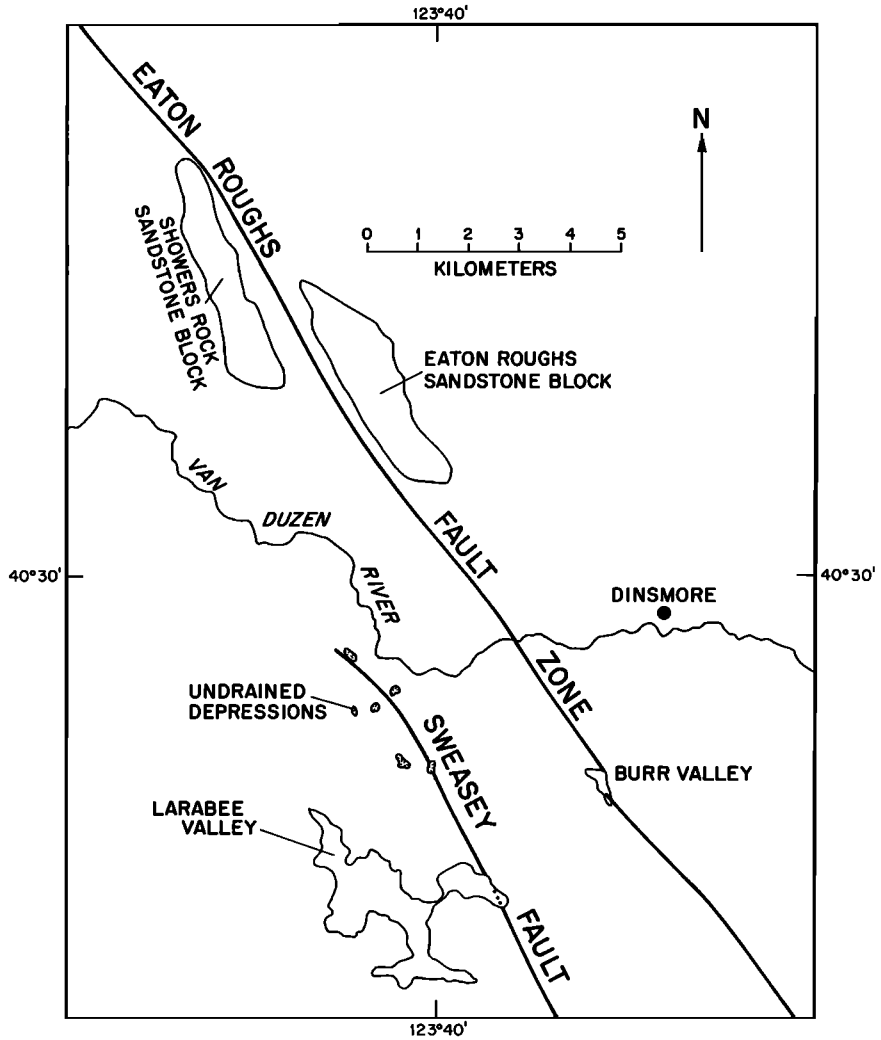

Fig. 9. Generalized geologic map of the Van Duzen River basin near Dinsmore, California, area showing the 3.3-km right-lateral offset of the lithologically similar Eaton Roughs and Showers Rock sandstone blocks. Entire map area is underlain by Franciscan assemblage sandstone or melange units. Alluvial valleys and undrained depressions of probably tectonic origin are also shown.

horizontal bedding creates a random pattern of the poles to planes, whereas the unrestored structural data show one or two clusters of poles to high-angle fault planes (Figure 5). From this we infer that the high-angle faults formed after folding. We found insufficient data to determine if the two clusters represented a conjugate set. However, nearly horizontal grooves and striations observed on some high-angle mesoscale fault planes near Maple Creek suggest that these structures are part of a system of strike-slip faulting.

Tectonic Transition at Northwest End of Eaton Roughs Fault Zone

Based on the mesoscale structural data, we infer that a transition in tectonic style occurs from contraction near the coast along the Mad River fault zone to translation inland along the Eaton Roughs fault zone. The transition occurs near Maple Creek (Figures 2 and 5).

Falor sediments along the Mad River fault zone are locally overturned in tight folds near the thrust faults. This overtuning is evident in the Falor near Maple Creek as well, where high-angle mesoscale faults are superimposed on the folds. From this relation we infer that inception of strike-slip faulting on the Eaton Roughs fault zone near Maple Creek is younger than inception of thrust faulting on the Mad River fault zone. If our interpretation is correct, high-angle faults of the Eaton Roughs fault zone near Maple Creek must cut earlier low-angle structures of the Mad River fault zone. Unfortunately, these relations are not exposed in the field. Farther northwest (toward the coast) along the Mad River fault zone, the two deformations are not superimposed. Hence right slip on the Eaton Roughs fault zone is probably occurring simultaneously with thrusting along the coastal portion of the Mad River fault zone.

A large component of translational displacement on the Eaton Roughs fault zone is probably being accommodated by contraction on the Mad River fault zone. Net horizontal shortening across the Mad River fault zone, from basement offset, is at least 3.6 km (see above). Lateral offset of the north-northwest trending Eaton Roughs from Showers Rock is about 3.5 km, suggesting that the Eaton Roughs fault zone in part accommodates northeast-southwest directed contraction. However, it is unlikely that all translational motion is dissipated in contraction on the Mad River fault zone, for three reasons. First, there are at least two strands (and possibly more) of the Eaton Roughs fault zone (Figure 3), and it is likely that right-slip displacement has occurred on multiple

strands. Second, 8 km north of Maple Creek, a subsiding basin called Murphy's Meadows (Figures 2, 3, and 5) occurs at a reasonable location for a pull-apart basin involved in the right step of deformation from the Eaton Roughs fault zone to faults of the Grogan fault zone. Third, the Prairie Creek sediments to the north-northwest have been offset by right-lateral translational strain that must be related to similar strain to the south-southeast. This strain is either being taken up on the Eaton Roughs fault zone or possibly on a southern (and poorly exposed) portion of the Grogan fault.

Transfer of strain north-northwestward from the Eaton Roughs fault zone to the Grogan–Lost Man fault system is attractive because northwest of Murphy's Meadows there are a series of prominent linear features on the west slope of the Redwood Creek basin that progressively step to the right to the Grogan fault, which offsets Prairie Creek sediments north of Orick, California [*Harden et al.*, 1982] (Figure 2). Along one of these linear features, the Bridge Creek lineament (BCL, Figure 2), a Pleistocene alluvial fill up to 50 m thick, is intensely fractured and faulted. The fractures are uniformly high angle, form a conjugate set, and have the same pattern as those adjacent to the Lost Man fault [*Kelsey and Cashman*, 1983], suggesting that faulting and some translational displacement have occurred along the Bridge Creek lineament during the Pleistocene.

Lake Mountain Fault Zone

The Lake Mountain fault zone was originally mapped by *Herd* [1978] as extending from near Covelo north-northwestward all the way to Maple Creek (Figure 3). We have subdivided the fault zone into the Lake Mountain fault zone and the Eaton Roughs fault zone because the fault pattern and the fault trend of the two fault zones are distinctively different. The change in pattern occurs near Kettenpom, California (K, Figure 3).

Evidence for both Holocene activity and right slip is more abundant for the Lake Mountain fault zone than for the Eaton Roughs fault zone. *Herd* [1978] first recognized the striking geomorphic evidence for youthful faulting along the Lake Mountain fault zone at Lake Mountain (LM, Figure 3). Abundant linear sag ponds, aligned drainages, topographic trenches, and saddles define four separate north trending, subparallel faults at Lake Mountain. Both to the north-northwest toward Zenia (Z, Figure 3) and to the south-southeast toward Round Valley (Figure 3), similar geomorphic features are present. Unlike the Eaton Roughs fault zone that consists of one or two well-defined continuous fault traces, individual faults on the Lake Mountain trend are more numerous, extend from 1 km to more than 30 km in length, and both left step and right step toward the north-northwest (Figure 3).

The transition from the Lake Mountain fault zone to the Eaton Roughs fault zone near Kettenpom entails a change in fault zone trend from N20°–25°W to N30°–35°W, respectively. The two fault zones overlap in the vicinity of the Kettenpom-Hoaglin valleys (KHV, Figure 3) and in the encompassing Salt Creek depression (SCD, Figure 3). The Salt Creek depression is an elongate, 40 km^2 topographic low. Drainage in the Salt Creek depression is anomalously toward the north-northwest (the master stream, the North Fork Eel River, flows south-southeast), and the depression has not undergone the regional uplift characteristic of the surrounding area. We feel that the depression is of tectonic origin and is due to localized extension in a 40 km^2 area associated with the change in fault trend and right step of the Lake Mountain fault zone northeastward to the Eaton Roughs fault zone. The elongate, roughly rhomboidal shape of the Salt Creek depression and its position in the fault zone are both features similar to other megascale depressions observed along dilational fault jogs in transcurrent fault systems [*Sibson*, 1986].

The Lake Mountain fault zone is the northward continuation of the Bartlett Springs fault zone, which was recognized by *McLaughlin and Nilsen* [1982] and *McLaughlin et al.* [1985*a*] to be a major fault zone of the San Andreas fault system. Earthquake focal mechanism solutions from seismicity along the Barlett Springs fault zone suggest right slip [*Dehlinger and Bolt*, 1984]. The fault zone offsets Quaternary sediments near Lake Pillsbury [*DePolo and Ohlin*, 1984]. *Clark* [1983] mapped 0.9 km of right-lateral offset for a distinctive Franciscan melange block along the Bartlett Springs trend and noted a series of small basins along the trend that he interprets as pull-apart basins related to right slip.

Our mapping of the Miocene Temblor Formation near Covelo indicates that these sediments may be offset right laterally about 2 km along a lineament at the southern end of the Lake Mountain fault trend (Figures 3 and 8). Though exposures are poor, the low-angle Temblor fault is apparently offset along the lineament. A megascale fold, seen in regional outcrop pattern and documented by bedding orientation in the eastern outcrop of Temblor sediment, probably developed during right slip (Figure 8). Fragments of Temblor sediment no more than 500 m^2 in area are smeared out in the Franciscan rocks near the fault trend between the two offset bodies of Temblor sediments (Figure 8). Offset of the Temblor places a maximum age of post-middle Miocene on the timing of faulting. However, because the offset occurs along the Lake Mountain trend, we infer that the offset is as young as latest Tertiary or Quaternary.

Garberville Fault Zone

The Garberville fault zone is a discontinuous series of north-northwest trending lineaments that extend south-southeast from Bull Creek, through Garberville, to just north of Laytonville (Figure 3). At its southern end the Garberville fault zone merges with the Maacama fault zone. In this region our fault lineament mapping overlaps by 16 km with that of *Pampeyan et al.* [1981], and there is good agreement on the location of major fault traces. There is no evidence of Holocene surface rupture along the Garberville fault; however, at least one surface rupture has occurred along the Maacama in Holocene time [*Upp*, 1982] and active right-lateral fault creep has been recorded on the northern section of the Maacama fault zone [*Harsh et al.*, 1978].

North-northwest of Garberville, the Garberville fault zone can be traced as a 4-km-long, north-northwest trending zone ($\sim$200 m wide) of sag ponds, notched ridges, and aligned springs (Figure 3). Intermittently, a well-defined trace is visible. Farther north, the Garberville fault zone in some manner probably connects to or offsets the Russ fault north of Cape Mendocino or the Capetown fault (Figure 2), though a lack of late Neogene or Quaternary cover sediments and an absence of well-defined lineaments prevent mapping this transition on aerial photographs. Near Garberville, the fault zone truncates the depositional base of the Garberville unit along a set of overlapping fault splays (Figure 6). One of these fault splays trends N70°W and dips 72°NE.

Due to the alignment of the Garberville fault zone with the Maacama fault zone to the south, it is likely that the Gar-

berville fault zone is an active, right-lateral fault system. The Garberville fault zone subparallels the coastal belt thrust [*Jones et al.*, 1978; *Underwood*, 1982] for most of its length. At two locations where the coastal belt thrust intersects one strand of the Garberville fault zone, apparent right-lateral offset of the coastal belt thrust of a few kilometers is implied (Figure 3). These offsets could be the result of right-lateral motion on the Garberville fault zone, but we have no field evidence to support this interpretation. An alternative interpretation (R. J. McLaughlin and S. Ellen, oral communication, 1987) is that the Garberville fault zone steps westward northwest of Garberville and is aligned with steep faults in the Franciscan coastal belt of that area (Figure 3). Therefore the nature of the northward continuation of the Garberville fault zone is speculative.

Near Garberville, mesoscale fractures and faults are well exposed in the Garberville unit at two river bank outcrops 100 and 400 m from the main fault trace. Analysis of these features shows high-angle fault clusters (Figure 7, sites C and D), and faults at site C form a conjugate pair. We infer that the high-angle mesoscale structures near the Garberville fault zone are genetically related to the fault zone and that the fault zone is high angle. If fractures are rotated to horizontal bedding (sites C and D, rotated versus unrotated, Figure 7), there is not a notable difference in the degree of clustering of pole-to-plane data. However, for the high-angle conjugate fault set (site C, Figure 7), rotation to horizontal bedding increases the proportion of low-angle (less than 45°) faults, thereby reducing the conjugate symmetry. Though field data are equivocal in this instance, we feel that the limited evidence suggests that the high-angle mesoscale structures formed after folding. In contrast, mesoscale structures associated with the Dean Creek fault are moderate to low angle and formed prior to folding (see discussion above).

The Dean Creek and Garberville faults, though subparallel in trend, are therefore inferred to have different dips and a different sense of movement based on associated mesoscale structures. Consequently, these faults probably represent two generations of faulting, the first in a contractional strain regime, the second in a translational strain regime.

An alternative possibility is that these low-angle and high-angle mesoscale fracture sets represent a single deformation event (i.e., the same tectonic stress field). Though mesoscale faults of different types can be due to a single tectonic stress state (*Angelier et al.* [1985] and *Frizzell and Zoback* [1987] cite field examples), we feel that this is unlikely at Garberville because the two mesoscale fault types are for the most part spatially separated and best developed adjacent to either one fault or the other.

Russ and Capetown Faults

Based on aerial photographs, both the Russ [*Ogle*, 1953] and Capetown faults appear to offset by approximately 70-m remnants of the most prominent late Pleistocene marine terrace surfaces at the coast near False Cape and Cape Mendocino, respectively (Figures 2 and 3). Mesoscale structures adjacent to the Russ fault are well exposed in a massive, subhorizontal 2-m-thick sand bed in Wildcat Group sediments [*Ogle*, 1953] along Wildcat Grade. The structures are moderately to steeply dipping (65°–90°), but no pattern is apparent, probably because of more than one generation of faulting.

We are uncertain of the sense of motion on these two faults because of the paucity of Neogene cover sediments in the vicinity. The principle compression axis in the North American plate near Cape Mendocino is north-south or northeast-southwest based on seismic records for 1972 [*Simila et al.*, 1975] or about N40°E as derived from historical geodetic data [*Snay et al.*, 1987]. *Simila* [1980, p. 134] states that the "inland shear zones near Cape Mendocino indicate strike-slip faulting" based on seismicity from 1968 to 1978. These observations suggest a strike-slip component to the Russ and Capetown faults, in addition to the vertical component indicated by the marine terrace elevations. A third component of crustal deformation is regional tilting, indicated by the southward tilt of the marine terrace remnants north of the Russ fault [*Ogle*, 1953]. If compression is north-south or northeast-southwest, then any strike-slip component on the east-west trending Russ and Capetown faults may be left lateral. However, movement on the Mendocino fracture zone due west offshore is right lateral [*McEvilly*, 1966]. The opposite senses of shear would imply weak coupling of the overriding and subducting plates near Cape Mendocino. If this is the case, the interaction of the two plates near Cape Mendocino is notably different from the strong plate coupling that is inferred near Humboldt Bay (see discussion below). Based on existing geodetic, seismological, and geologic data, therefore, it is inconclusive whether the Cape Mendocino area is primarily deforming by lateral or compressional strain. We suspect that the former is dominant, but it is unclear whether lateral strain on mapped faults in this region is dextral or sinistral. Additional work on the neotectonics of the area just north and east of Cape Mendocino is clearly needed.

San Andreas Fault Zone

We did not investigate the San Andreas fault zone because the fault zone is offshore in northern California. A possible exception is an onshore fault segment at Point Delgada where tectonic ground rupture occurred during the 1906 earthquake [*Brown and Wolfe*, 1972]. Based on the dating of adularia veins that cross the supposed fault trace, however, *McLaughlin et al.* [1985*b*] concluded that tectonic offset may not have occurred in 1906 at Point Delgada.

Net right-lateral offset along the combined San Andreas–Hosgri–San Gregorio fault trends since post-early Miocene is approximately 440 km (*Fox et al.* [1985], compiled from numerous studies). Net right-lateral slip on the Eaton Roughs–Lake Mountain fault zone, and possibly the Garberville fault zone, is minor (< 5 km) compared to late Neogene right slip on the San Andreas. However, right-slip rates on these three fault zones in the last 0.1 m.y. may be comparable.

SPATIAL PATTERN OF CONTEMPORANEOUS DEFORMATION

Deformation in northern coastal California consists of a forearc contractional zone, characterized by thrust faults and associated folds, and a zone of lateral translation, characterized by right-lateral strike-slip faults (Figure 10). The northern portion of the translation zone is within the forearc and overlies the subducted Gorda slab. The southern portion of the translation zone overlies the slab window and is the northernmost segment of the transform boundary between the North American and Pacific plates (Figure 10). Of the three distinct right-lateral fault zones that make up the northernmost part of the transform boundary, the two western fault zones (but not the San Andreas fault zone) continue to be well defined tens of kilometers northward into the forearc.

The eastern boundary of the translational zone is taken to

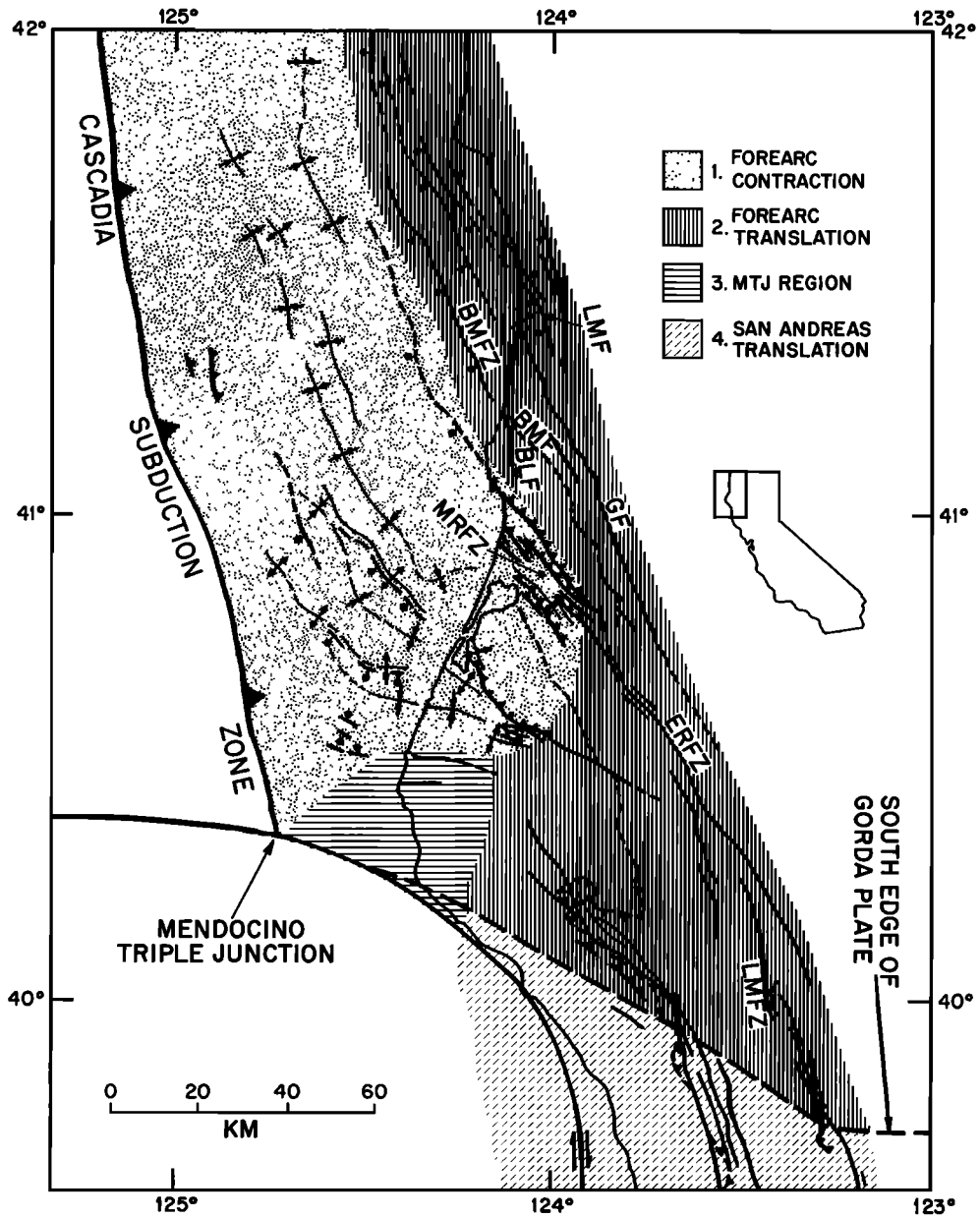

Fig. 10. Tectonic map of California showing the extent of contractional and translational zones. Offshore data from *Clarke* [1987]. Region 1, zone of forearc contraction; region 2, zone of forearc translation; region 3, zone of translation within the San Andreas transform zone; region 4, Mendocino triple junction region. See text for further explanation. LMFZ, Lake Mountain fault zone; ERFZ, Eaton Roughs fault zone; GF, Grogan fault; BMF, Bald Mountain fault; BLF, Big Lagoon fault; LMF, Lost Mountain fault; BMFZ, Bald Mountain fault zone. South edge of Gorda plate after *Jachens and Griscom* [1983] and *Wilson* [1986].

be the easternmost limits of the combined Lost Man–Grogan–Eaton Roughs–Lake Mountain fault zones, which together define the eastern limit of distinct linear features and landforms associated with youthful faulting. Farther to the east, pronounced north-northwest linear features persist in the landscape, but they are not associated with the Quaternary landforms characteristic of recently active faults. The northern extent of translation is unknown, but translational deformation on land narrows toward the coastline to a 10-km-wide belt at the mouth of the Klamath River (KRM, Figure 2).

On the basis of structural mapping on the continental shelf [*Clarke*, 1987], we correlate mapped faults on land to offshore structures (Figures 10 and 11). Faults that are correlatable with the Lost Man, Grogan, Bald Mountain, and Big Lagoon faults appear on acoustic reflection profiles to be steeply east dipping to vertical [*Clarke*, 1987] (Figures 10 and 11). The faults extend to or near the seafloor and offset Quaternary sediments. Basement offsets suggested by the acoustic reflection data are 100–1300 m up to the northeast [*Clarke*, 1987]. Right slip is suggested along the faults by their steep dips, relatively straight traces, variation in amount of apparent offset along the traces, and en echelon folds associated with the fault traces [*Clarke*, 1987].

The contact between the contraction and translation zones is moderately well defined both onland and offshore. The contraction-to-translation transition on the continental shelf is within a north-northwest trending transition zone between the Trinidad fault zone and the Bald Mountain fault zone

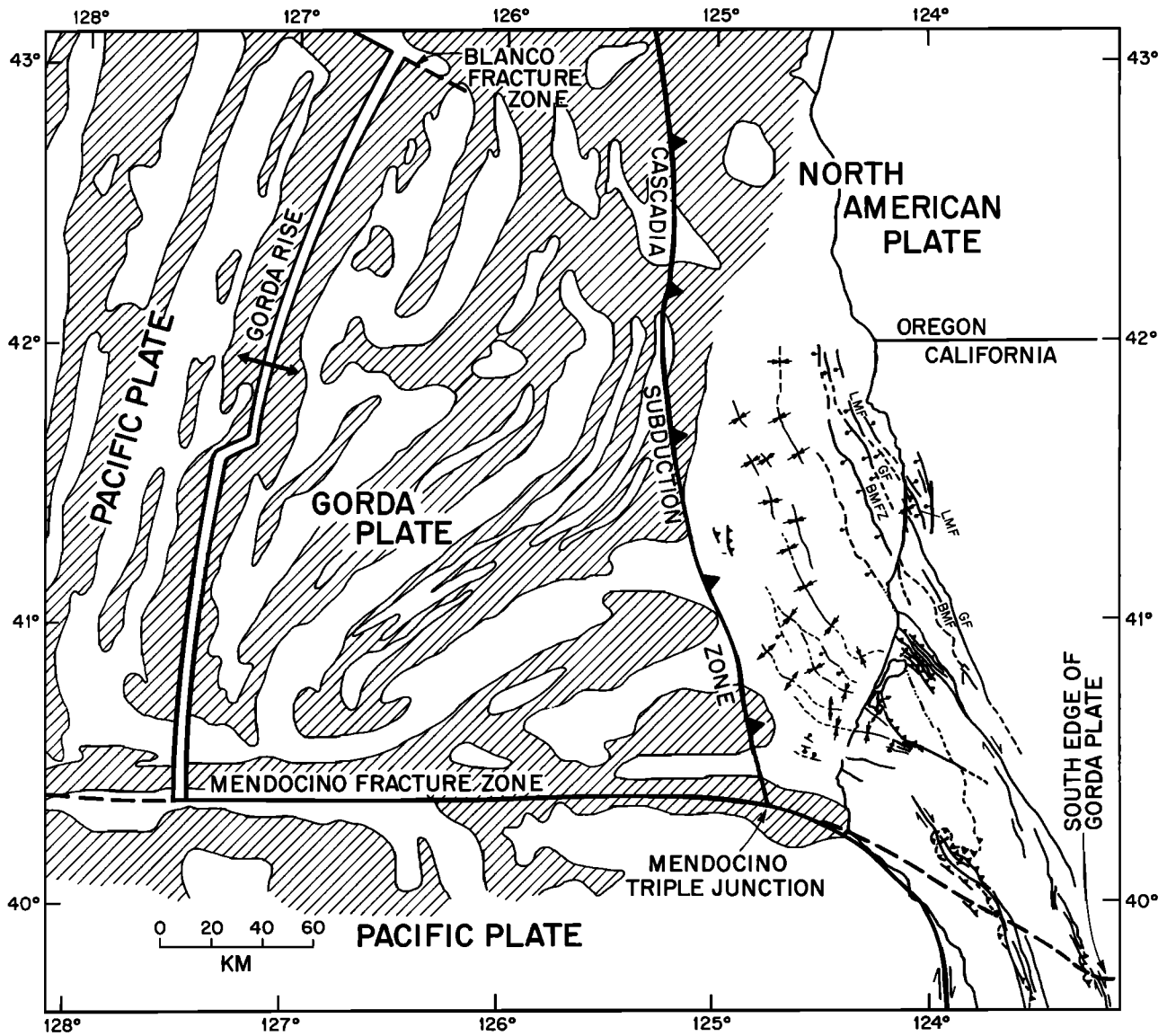

Fig. 11. Tectonic map of north coastal California (from Figure 2) shown in context of the Pacific, Gorda, and North American plate boundaries and the deformation of the magnetic anomalies in the south Gorda plate. Magnetic data and south edge of Gorda plate from Figure 6 of *Jachens and Griscom* [1983]. Offshore structure data from *Clarke* [1987].

[*Clarke*, 1987] (Figure 11). From the latitude of Big Lagoon (BL, Figure 2), the transition boundary heads north-northwestward, then northward, and by the latitude of the Klamath River, it is subparallel to the coastline about 30–35 km offshore.

On land, this transitional contact defines a semicircular area of contraction centered about Humboldt Bay. The onshore and offshore data combined therefore suggest that the zone of contraction resulting from Gorda–North American plate is widest just north of Cape Mendocino in the vicinity of Humboldt Bay (Figure 10). The transition between contraction and translation is well defined for the Eaton Roughs–Mad River fault zone. However, the northern end of this on-land transition is poorly defined. Little is known about either the Big Lagoon or Bald Mountain faults. The Big Lagoon fault offsets and folds late Neogene and Quaternary sediments near Big Lagoon. The straight trace suggests that the Big Lagoon fault is high angle (Figure 2), though mesoscale structural data near the fault are not available. The Bald Mountain fault nowhere offsets Neogene or younger sediments. The fault appears to be high angle within 5 km of the coast [*Cashman et al.*, 1986], but the sinuous outcrop trace of the fault suggests that it may not be high angle farther inland (Figure 2).

To the south, the contractional zone is bounded by the Mendocino triple junction region (Figure 10). This area shows evidence of both late Pleistocene faulting and broad crustal tilting. The sparse data provided from seismicity [*Simila et al.*, 1975; *Simila*, 1980] and from field study of the Russ and Capetown faults suggest that translation dominates the deformational style.

Maps showing epicentral distribution of seismicity for the area roughly encompassed by Figures 2 and 3 for the period 1980–1982 [*Cockerham*, 1984; *Walter*, 1986] show a pattern of shallow depth earthquakes that, in a broad sense, reflect mapped translational faults on the northern part of the San Andreas transform zone. The most striking correspondence is the two pronounced north-northwest linear trends of epicenters that correspond to the Maacama and Bartlett Springs

fault zones. Near latitude 39°50'N, seismicity is also prevalent along the southernmost mapped traces of the Garberville and Lake Mountain fault zones. However, seismicity does not reflect these two mapped fault traces farther north (north of latitude 40°N) in the zone of forearc translation.

Seismicity is frequent but scattered beneath the contractional zone south and southeast of Humboldt Bay [*Walter*, 1986]. Most earthquakes occur at a depth of 10–30 km. This broad zone of seismicity dies out to the north and east [*Smith and Knapp*, 1980; *McPherson et al.*, 1981], and the coastal portion of the Mad River fault zone shows a low level of seismicity. In general, seismicity in the contractional zone cannot be related to mapped surface faults, despite much evidence of Quaternary faulting. The scattered hypocenters in the contractional zone may in part reflect diffuse seismicity on the shallow dipping thrust faults. However, the depth of the hypocenters [*Walter*, 1986] suggests that most of the broad seismicity in the contraction zone reflects subduction and internal breakup of the Gorda plate at depth. Because the thrust faults do not manifest frequent seismicity (they have been historically quiescent), they must release stress more infrequently in large, shallow focus earthquakes. The recurrence interval of faults with late Pleistocene scarps in the vicinity of Humboldt Bay [*Woodward-Clyde Associates*, 1980] supports this contention.

Seismicity decreases to the east of Humboldt Bay and the contraction-to-translation transition occurs above the region where, at depth, the south-eastward dip of the Benioff-Wadati zone notably steepens [*Cockerham*, 1984; *Walter*, 1986].

TIMING OF DEFORMATION

Faunal ages aid in constraining the timing of deformation of the Neogene sedimentary units. The southernmost unit, the Temblor Formation, is middle Miocene on the basis of fossil teeth and oysters [*Clark*, 1940]. Deposition of the Garberville sediments (the next Neogene unit to the north) spans the interval late-early-to-middle Miocene for the Kimtu unit and late Miocene to Pliocene for the Garberville unit [*Menack*, 1986]. *Menack* [1986] cites evidence for minor syndepositional uplift and tilting of just the Garberville unit, but the general uniform dip of both the Kimtu and Garberville units of 15°–40° northwest (Figure 6) suggests that the major episode of contractional deformation occurred after the last phase of deposition in the late Pliocene (about 2–3 Ma) but before onset of translational deformation related to the Garberville fault zone. The upper Garberville unit is a regressive sequence [*Menack*, 1986], and we infer that deposition in the Garberville unit ceased due to uplift and contraction of the basin in a fashion similar to the tectonic demise of the Falor basin.

Falor Formation deformation probably did not commence until about 0.7 Ma for reasons discussed above. Contractional deformation of the Falor Formation is at least as recent as latest Pleistocene and probably is active.

The late Neogene and Quaternary tectonic history of the Temblor and Garberville sediments is similar and consists of (1) a period of contractional deformation following deposition in which the units were folded and thrust under Franciscan sediments, and (2) subsequent right-lateral deformation. Deformation in the Falor is constrained to within the last 1 m.y. Major deformation of the Garberville sediments commenced after about 2–3 m.y. Deformation in the Temblor Formation is not geologically constrained, except as younger than the faunal age of this unit. Faunal ages of the Temblor and Garberville sediments overlap in the middle Miocene, but Temblor deposition terminated in the Miocene and deposition of the Garberville unit persisted until at least the late Pliocene. Thus these sedimentary packages tend to become younger to the north.

DISCUSSION

Pattern of Deformation

Late Neogene and Quaternary crustal deformation in northern coastal California is divided into two strain regimes: contraction and lateral translation. Lateral translation occurs along the San Andreas fault system above the slab window south of the subducted Gorda plate. Strike-slip faulting also occurs in the forearc region north of the triple junction as a linear zone (8–15 km wide) arcward of the contracting wedge of sediment at the continental margin. This thin zone, which includes the Eaton Roughs–Grogan–Lost Man fault zone, is typical of transcurrent fault zones within the forearc region landward of obliquely convergent subduction zones [*Fitch*, 1972; *Jarrard*, 1986]. The forearc strike-slip fault system connects to the south with faults of the San Andreas fault system. The forearc faults do not exhibit the abundant microseismicity characteristic of those translational faults to the south above the slab window. As the slab window migrates northward, these forearc strike-slip faults will probably become the active faults of the San Andreas transform plate boundary, as suggested by *Kelsey and Cashman* [1983]. Geologic data, presented above, show that the forearc strike-slip faults have offset Pleistocene Falor and Prairie Creek sediments and they are probably active faults despite the lack of microseismicity along their traces.

As dictated by plate convergence, contraction occurs in the forearc region immediately landward of the subduction zone. The Dean Creek thrust fault and the Temblor fault also record contraction, but these faults are presently south of the Mendocino triple junction, near the northern margin of the slab window, and well within the San Andreas fault system. We infer that this contraction predates San Andreas right-slip motion.

Herd [1978] suggested that right-slip faults of the San Andreas fault system north of San Francisco Bay defined the sliver-shaped Humboldt plate, which is moving northward relative to stable North America. Based on our fault mapping and limited offset data, we do not see evidence for a rigid plate. The sliver appears to be internally deforming by right slip on the Maacama and Garberville fault zones at rates approximately equal to right slip on the east margin of the sliver along the Bartlett Springs–Lake Mountain–Eaton Roughs fault zones. Perhaps deformation across the Humboldt plate between latitudes 39°45'N and 40°15'N (Figure 3) is similar to that suggested by *Prescott and Yu* [1986] for the region immediately north of San Francisco Bay, where plate motion is distributed over a wide zone. Thus the Humboldt plate, better called the Humboldt deformation zone, is an elongate zone internally deforming by right slip and also being displaced by right slip from stable North America. There are compelling arguments based on lithospheric strength [*Vink et al.*, 1984] and subduction geometry [*Jarrard*, 1986] that continental slivers such as the Humboldt deformation zone can become detached and migrate great distances as displaced terranes. The Humboldt deformation zone may therefore be an incipient terrane sliver just starting (or continuing) its voyage northward.

Mechanism of Upper Plate Deformation Near Humboldt Bay

The southernmost part of the zone of forearc contraction at Humboldt Bay spatially coincides with the southeastern portion of the subducted Gorda plate (Figure 11). This is the portion of the Gorda plate that is undergoing maximum internal distortion, based on both an elastic model of *Jachens and Griscom* [1983] and a kinematic strain rate model of *Wilson* [1986]. The internally deforming downgoing slab is underneath the wide southernmost portion of the upper plate zone of contraction (Figure 11). We feel that this spatial overlap is best explained by coupling of the downgoing and deforming Gorda plate with the overriding North American plate. This coupling is reflected in surface faulting by a rapid rate of North American plate contraction in the last 1 m.y. (a minimum of 5.2 mm/yr of NE-SW shortening on the Mad River fault zone and a minimum of 1.3 mm/yr of NE-SW shortening on the Little Salmon fault system) and in the fact that microseismicity in recent years (1974–1977, 1981–1982) is high in the vicinity of Humboldt Bay but dies off rapidly to the east of longitude 124° [*Smith and Knapp*, 1980; *Cockerham*, 1984]. The inferred translational deformation on the Russ and Capetown faults may also reflect upper plate coupling to the lower plate, in which case the translational strain is right lateral, consistent with the sense of motion between the Gorda and Pacific plates along the Mendocino fracture zone to the west [*Couch*, 1980]. Conversely, if coupling is not strong near Cape Mendocino, the documented northeast-southwest contraction in the North American plate requires that any translation along the Russ or Capetown faults be left lateral.

Seismic Hazard in Humboldt Bay

Gorda-North American plate coupling and the resulting significant amounts of shortening in the North American plate have implications for seismic hazard in the Humboldt Bay area. A minimum value for the total northeast-southwest directed shortening in the contraction zone is 7.9 mm/yr in about the last 0.7–1.0 m.y. This rate is between 25 and 100% of the total convergence rate between the Gorda and North American plates in the last 5 m.y. or less, depending on the time period and whether one employs the convergence values and azimuths of *Riddihough* [1984] or *Engebretson et al.* [1985]. In either case, contraction in the North American plate has accommodated a significant amount of the strain associated with subduction. This in turn must decrease the amount of potential stress buildup that could occur within the subduction zone on the megathrust. Stress released in thrust fault events within the forearc in the southernmost portion of the Cascadia subduction zone near Humboldt Bay may be substantial [*Carver and Burke*, 1987]. Though geologic and seismotectonic data suggest a potentially great seismic hazard for the rest of the Cascadia subduction zone [*Heaton and Hartzell*, 1987; *Atwater*, 1987], it remains unclear whether the thrust faults of the Humboldt Bay area pose a greater or lesser seismic hazard than rupture along a portion of the megathrust further north along the Cascadia subduction zone.

Kinematic Model for Deformation Associated With Triple Junction Migration

If the relatively wide part of the forearc contraction zone around Humboldt Bay reflects subduction of an internally deforming Gorda plate, then this wide contractile zone should have existed at the inception of internal deformation of the Gorda plate, about 3 Ma [*Wilson*, 1986]. Further, the wide contractile zone must migrate northward at the rate of migration of the Mendocino triple junction in the last 3 m.y. In a longitudinal frame of reference this migration was about 30.3 arc min of latitude/m.y. (about 56 km/m.y.) [*Engebretson et al.*, 1985].

Based on the above triple junction migration rate and inferences on the mechanism of deformation, we suggest that sequential episodes of contractional and translational deformation of the Temblor Formation and the Garberville sediments can be spatially and temporally correlated with the passage to the west of the Mendocino triple junction and the northward migration of the slab window. The timing for this kinematic model is based on the inference that, first, Falor Formation sediments at the northern edge of the contraction zone started to deform sometime between 0.7 and 1.0 Ma, when the Mendocino triple junction was 56–63 arc min of latitude (104–117 km) south of the latitude of the Falor Formation (we assume here that North America is fixed in the geographic reference frame). Second, the Eaton Roughs fault zone propagated northward and offset the Falor Formation sometime within the last 0.1–0.01 m.y.

In a similar fashion the Garberville sediments and the Temblor Formation must have started to deform when the Mendocino triple junction was about 104–117 km south of each of these sedimentary units, respectively. At a migration rate of about 56 km/m.y., deformation would have started approximately 1.8–2.1 m.y. before the Mendocino triple junction arrived at the latitudes of these units. Given that the Garberville and Temblor sediments were opposite the triple junction at 0.4 and 1.2 Ma [*Engebretson et al.*, 1985], these units started to deform at about 2.2–2.5 and 3.0–3.3 Ma, respectively (Table 3), given our tectonic model. Figure 12 is a schematic portrayal of the model, showing one possible reconstruction of triple junction location along the California coast at the times when the Temblor, Garberville, and Falor sediments, respectively, started to deform.

The 3.0–3.3 Ma time for inception of contractional faulting in the Temblor Formation is close to the 3 Ma time when Gorda-Pacific relative plate motion changed, initiating subduction of a deforming Gorda plate. Contraction therefore should not be an important deformational event for Neogene sediments south of the Temblor Formation.

Neogene sediments of the Little Sulphur Creek basins occur farther south at latitude 38°45'N. The sediments are exposed along the trend of the Maacama fault and were deposited in a pull-apart basin [*McLaughlin and Nilsen*, 1982]. These basins formed and were syntectonically filled in an extensional environment related to the passage of the Mendocino triple junction to the west at approximately 3–4 Ma [*McLaughlin and Nilsen*, 1982]. The extensional regime probably was due to instabilities inherent in the migration of the triple junction [*Dickinson and Snyder*, 1979*a*], at a time prior to the relative motion change between the Gorda and the Pacific plates. By the time the triple junction migrated to a latitude about 59 arc min south of the Temblor sediments and 15 arc min south of the Sulphur Creek basins (39°00'N), however, relative plate motion had changed, and deformation to the northeast of the triple junction was contractional rather than extensional.

Reconstruction of Deformation in Northern California in the Last 3 m.y.

Based on our kinematic model, we present a speculative reconstruction of the timing and distribution of crustal deformation in north coastal California in the last 3 m.y. (Table 3).

TABLE 3. Timing of Deformation in North Coastal California Related to Northward Migration of Triple Junction

Sedimentary Unit	Latitude of Unit	Estimated Age of Unit[a]	Start of Contractional Faulting, Ma	Start of Strike-Slip Faulting, Ma
Falor Formation	40°53'N	early Pleistocene	0.7–1.0[b]	0.1 – .01[c]
Garberville sediments	40°08'N	late-early Miocene to Pliocene	2.2–2.5[b]	1.3–1.6[c]
Temblor Formation	39°45'N	middle Miocene	3.0–3.3[c]	2.1–2.4[c]

[a]Ages of units discussed in text.
[b]Timing of deformation is constrained by geologic evidence (see text).
[c]Timing of deformation is interpreted from proposed tectonic model, no geologic age constraints are available (see text).

The wide forearc contractile zone at the south end of the Cascadia subduction zone migrates northward in front of the triple junction and precedes arrival of the triple junction to the west by about 2 m.y. Translational deformation follows in the wake of contractional deformation by about 0.9–1.0 m.y., based on the timing of inception of translational deformation in the Falor Formation near Maple Creek. This translational deformation, which is superimposed on initial contraction, commences in a forearc setting but persists as the slab window migrates northward into the position previously occupied by the downgoing slab. Projections of the edge of the Gorda plate under North America, inferred from gravity data and plate motions [*Jachens and Griscom*, 1983; *Wilson*, 1986] (Figures 10 and 11), indicate that the slab edge is presently approximately below the Temblor Formation. We therefore infer that the slab window arrives about 3 m.y. after contraction starts, or 2 m.y. after strike-slip faults start to be superimposed on top of the contraction in the forearc.

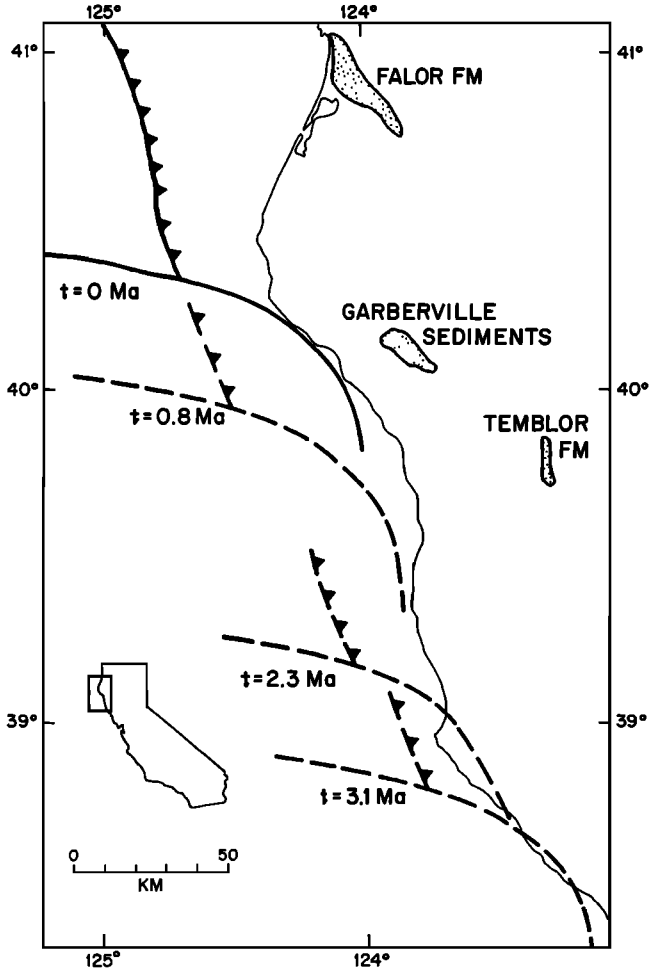

Fig. 12. Map of west coast of California showing three previous positions of Mendocino triple junction. The reconstructed positions are for the three approximate times (3.1., 2.3, and 0.8 Ma) at which the Temblor Formation, Garberville sediments, and Falor Formation, respectively, started to deform in response to the northwardly migrating triple junction. Migration rate from *Engebretsen et al.* [1985].

The superposition of strike-slip faulting on reverse faulting, observed at both Garberville and near Covelo, will occur in the Mad River fault zone in the next 1–1.5 m.y. as the Eaton Roughs fault zone propagates through and dominates over the thrusts of the Mad River fault zone. Similarly, the Garberville fault zone may propagate through the contractile fault zones (Little Salmon fault, Goose Lake faults) that presently exist south of Humboldt Bay. Alternatively, right-slip motion on the Garberville fault zone may cease as the neighboring Eaton Roughs fault zone becomes dominant. Because of the northerly trend of the subduction zone that favors right stepping of the transform boundary [*Dickinson and Snyder*, 1979*b*], we favor the latter option.

A further implication of this tectonic scenario is that the contractional structures observed near Covelo and Garberville probably represent a small fraction of the total number of thrust faults and associated folds that must have developed in the forearc as the subducting and deforming Gorda plate migrated northward. Only where Neogene sediments are not stripped away by erosion is evidence for this contraction preserved. In the Mad River fault zone, where erosion is less advanced, numerous folds and imbricate thrust faults are exposed.

Deformation in the Garberville sediments supports the notion that the King Range terrane of *McLaughlin et al.* [1982] was accreted to North America farther to the south, perhaps at the latitude of the Transverse Ranges, and brought northward by the San Andreas fault and obductively accreted in the latest Neogene, as suggested by *McLaughlin et al.* [1985*b*]. The Garberville sediments do not record a mid-Miocene contractional event of the magnitude that should be observed if the King Range was obductively accreted at the latitude where it is now. However, the sediments do show strike-slip deformation that is reasonably compatible with a late Neogene strike-slip docking of a terrane traveling to the north-northwest.

CONCLUSIONS

Strain patterns within the forearc at a convergent margin adjacent to a passing triple junction show a systematic evolution with time. The pattern of late Neogene and Quaternary deformation in northern coastal California (Figure 10) is consistent with a model of deformation that takes into account (1) the northward migration of the Mendocino triple junction and the San Andreas transform boundary, (2) internal deformation of the Gorda plate in the last 3 m.y., and (3) substantial contraction in the overriding North American plate in the last 3 m.y. due to subduction of the internally deforming Gorda plate.

The model of deformation is based on mapping of deformational structures in northern coastal California (Figures 2

and 3); these structures show evidence of crustal contraction or translation or both. North of the slab window (as defined by *Dickinson and Snyder* [1979*b*]), where the Gorda plate is subducting beneath North America, deformation in the North American forearc consists of a 30-km-wide zone of on-land contraction with a narrower zone of translation farther to the east (Figure 2). The zone of on-land contraction is the subaerial portion of the relatively wide southernmost extent of contractional deformation in the forearc of the Cascadia subduction zone (Figure 10). Thrust faults and associated folds of the Mad River and Little Salmon fault zones are the principle contractional structures. Strike-slip faults of the Eaton Rough fault zone are the translational structures farther to the east. Net northeast-southwest directed contraction across the Mad River fault zone in the Quaternary is at least 3.6 km, and minimum fault slip rates on the five thrust faults in the zone range from 0.8 to 2.3 mm/yr. The net slip rate across the Mad River thrust fault zone is at least 6.4 mm/yr (Table 1). A minimum slip rate estimate for the Little Salmon fault during the Pleistocene is about 2 mm/yr, and net northeast-southwest directed contraction across the Little Salmon fault is at least 4.3 km (computed from data of *Woodward-Clyde Associates* [1980]). Net right slip on the Eaton Roughs fault zone is uncertain, but limited geologic evidence suggests that it is of the order of 3 km.

Farther south above the slab window (Figure 10), translation presently is the predominant type of deformation. This translation is accommodated along two major right-lateral fault systems of the San Andreas transform boundary, the Lake Mountain and Garberville fault zones (Figure 3). However, discontinuous exposures of late Neogene sediments along these fault zones near Covelo and Garberville, California, respectively, indicate that a period of crustal contraction, expressed by thrust faults and associated folding, predated the present translational deformation (Figures 6 and 8). The earlier period of contractional deformation originated in the southern outcrop area of Neogene sediments (the Temblor Formation near Covelo), and contractional deformation started at a later date in the Garberville sediments. Translational movement along the Lake Mountain and Garberville fault zones truncates the earlier contractional structures.

Constraints on the timing of initiation of contraction in the Temblor and Garberville sediments (Table 3) suggest that inception of contraction was related to both migration of the triple junction and to a major change in plate motion between the Pacific and Gorda plates at about 3 Ma [*Wilson*, 1986]. Late Neogene contraction is not observed in Neogene sediments south of the Temblor sediments because Neogene sediments south of the Temblor were deformed prior to 3 Ma. Assuming coupling of the Gorda plate to the overriding plate, internal deformation of the Gorda plate promoted contraction in the North American plate. This contractional welt migrated northward in the forearc of the North American plate in advance of the Mendocino triple junction and at the rate of migration of the triple junction. The position of the tripe junction at the times of initial contraction in the Temblor and Garberville sediments (Figure 12) is determined based on the present configuration of the triple junction relative to active deformation farther north in the Humboldt Bay area and on the assumption that this deformation is genetically related in space and time to the present position of the triple junction.

Present-day deformation in the vicinity of Humboldt Bay therefore consists of contractional deformation associated with subduction of the Gorda plate and translational faulting farther to the east associated with oblique convergence at the Gorda–North American plate boundary. As the Mendocino triple junction migrates farther northward and the San Andreas transform boundary extends in length, the strike-slip faults of the San Andreas will extend to the north-northwest into the present forearc, and forearc strike-slip fault zones such as the Eaton Rough fault zone will become faults of the San Andreas fault system. Concurrently, the contractional structures near Humboldt Bay (Mad River fault zone and Little Salmon fault) will cease to be active and will be preserved in the geologic record in the same way as contractional structures are preserved in Neogene sediments farther south near Covelo and Garberville.

Acknowledgments. T. A. Stephens contributed substantially to field mapping in the Mad River fault zone. Kelsey's mapping in the Temblor Formation was facilitated by logistical help from the U.S. Geological Survey and the field assistance of F. Hochstaeder. J. C. Young provided valuable field data for both the Falor and Prairie Creek formations. Soil investigations by Bud Burke contributed to neotectonic interpretations. C. M. de Polo generously gave permission to use a fault map compilation that forms the basis of Figure 1. R. J. McLaughlin lent us a preliminary copy of his mapping on the Garberville and Covelo 1° sheets. The trace of the coastal belt thrust in Figure 3 is taken with permission from unpublished mapping of R. J. McLaughlin, S. Ellen, A. Jayko, and M. C. Blake. S. H. Clarke provided comment on our onshore-offshore fault correlations. R. F. Burmester aided with statistical analysis of fault data. R. L. Wheeler guided us to a more rigorous presentation of mesoscopic fault data. Research was supported in part by U.S. Geological Survey Earthquake Hazard Reduction Program contract 14-08-0001-22009. S. M. Cashman, R. J. McLaughlin, D. J. Merritts, R. S. Stein, J. C. Tinsely, and R. S. Yeats reviewed the manuscript.

REFERENCES

Angelier, J., Tectonic analysis of fault slip data sets, *J. Geophys. Res.*, *89*, 5835–5848, 1984.

Angelier, J., B. Colletta, and R. E. Anderson, Neogene paleostress changes in the Basin and Range, *Geol. Soc. Am. Bull.*, *96*, 347–361, 1985.

Atwater, B. F., Evidence for great Holocene earthquakes along the outer coast of Washington state, *Science*, *236*, 942–944, 1987.

Atwater, T., Implication of plate tectonics for the Cenozoic tectonic evolution of western North America, *Geol. Soc. Am. Bull.*, *81*, 3513–3536, 1970.

Blake, M. C., Jr., and D. L. Jones, The Franciscan assemblage in northern California: A reinterpretation, in *The Geotectonic Evolution of California*, Rubey vol. 1, edited by W. G. Ernst, pp. 306–328, Prentice-Hall, Englewood Cliffs, N. J., 1981.

Blake, M. C., R. H. Campbell, T. W. Dibblee, D. G. Howell, T. H. Nilsen, W. R. Normark, J. C. Vedder, and E. A. Silver, Neogene basin formation in relation to plate-tectonic evolution of the San Andreas fault system, California, *Am. Assoc. Pet. Geol. Bull.*, *62*, 344–372, 1978.

Blake, M. C., Jr., A. S. Jayko, and R. J. McLaughlin, Tectonostratigraphic terranes of the northern Coast Ranges, California, in *Tectonostratigraphic Terranes of the Circum-Pacific Region, Earth Sci. Ser.*, vol. 1, edited by D. G. Howell, pp. 159–171, Circum-Pacific Council for Energy and Mineral Resources, Houston, Tex., 1985.

Bloom, A. L., W. S. Broecker, J. M. A. Chappell, R. K. Matthews, and K. J. Mesolella, Quaternary sea level fluctuations on a tectonic coast: New $^{230}Th/^{234}U$ dates from the Huon Peninsula, New Guinea, *Quat. Res.*, *4*, 185–205, 1974.

Brown, R. D., Jr., and E. W. Wolfe, Map showing recently active breaks along the San Andreas fault between Point Delgada and Bolinas Bay, California, *U.S. Geol. Surv. Misc. Field Invest. Map, I-681*, 1972.

Bull, W. B., Correlation of flights of global marine terraces, in *Tectonic Geomorphology*, edited by M. Morisawa and J. T. Hack, pp. 129–154, Allen and Unwin, Winchester, Mass., 1985.

Burke, R. M., G. A. Carver, and S. Lundstrom, Soil development as a relative dating and correlation tool on marine terraces of northern California (abstract), *Geol. Soc. Am. Abstr. Programs*, *18*, 91, 1986.

Carver, G. A., and R. M. Burke, Late Holocene paleoseismicity of the southern end of the Cascadia subduction zone, *Eos Trans. AGU*, *68*, 1240, 1987.

Carver, G. A., T. A. Stephens, and J. C. Young, Quaternary thrust and reverse faulting on the Mad River fault zone, coastal northern California (abstract), *Geol. Soc. Am. Abstr. Programs, 15*, 316, 1983.

Carver, G. A., R. M. Burke, and H. M. Kelsey, Deformation of late Pleistocene marine terraces along the California coast north of Cape Mendocino (abstract), *Geol. Soc. Am. Abstr. Programs, 18*, 93, 1986.

Cashman, S. M., P. H. Cashman, and J. D. Longshore, Deformational history and regional tectonic significance of the Redwood Creek schist, northwestern California, *Geol. Soc. Am. Bull., 96*, 35–47, 1986.

Cashman, S. M., H. M. Kelsey, and D. R. Harden, Geology and descriptive geomorphology of the Redwood Creek basin, Humboldt County, California, Geomorphic Processes and Aquatic Habitat in the Redwood Creek Basin, Northwestern California, edited by K. M. Nolan, H. M. Kelsey, and D. C. Marrou, *U.S. Geol. Surv. Prof. Pap., 1454*, in press, 1988.

Chappell, J. M. A., A revised sea level record for the last 300,000 years on Papua New Guinea: A numerical calculation, *Quat. Res., 9*, 265–287, 1983.

Clark, J. T., Geology of the Bartlett Springs trend, northern Coast Ranges, California, M.S. thesis, 68 pp., Univ. of Tex. at Austin, Austin, 1983.

Clark, S. G., Geology of the Covelo district, Mendocino County, California, *Univ. Calif. Berkeley Publ. Geol. Sci., 25*, 119–142, 1940.

Clarke, S. H., Geology of the California continental margin north of Cape Mendocino, in *Geology and Resource Potential of the Continental Margin of Western North America and Adjacent Ocean Basins—Beaufort Sea to Baja California, Earth Sci. Ser.*, vol. 6, edited by D. W. Scholl, D. W. Grantz and J. G. Vedder, pp. 15A1–15A8, Circum-Pacific Council for Energy and Mineral Resources, Houston, Tex., 1987.

Cockerham, R. S., Evidence for a 180-km-long subducted slab beneath northern California, *Bull. Seismol. Soc. Am., 74*, 569–576, 1984.

Couch, R., Seismicity and crustal structure near the north end of the San Andreas fault system, Studies of the San Andreas Fault Zone in Northern California, edited by R. Streitz and R. Sherburne, *Spec. Rep. Calif. Div. Mines Geol., 140*, 139–151, 1980.

Dehlinger, P., and B. A. Bolt, Seismic parameters along the Bartlett Springs fault zone in the Coast Ranges of northern California, *Bull. Seismol. Soc. Am., 74*, 1785–1798, 1984.

DePolo, C. M., and H. N. Ohlin, The Bartlett Springs fault zone: An eastern member of the California plate boundary system (abstract), *Geol. Soc. Am. Abstr. Programs, 16*, 6, 486, 1984.

Dickinson, W. R., and W. S. Snyder, Geometry of triple junctions related to San Andreas transform, *J. Geophys. Res., 84*, 561–572, 1979*a*.

Dickinson, W. R., and W. S. Snyder, Geometry of subducted slabs related to San Andreas transform, *J. Geol., 87*, 609–627, 1979*b*.

Engebretson, D. C., A. Cox, and R. G. Gordon, Relative motions between oceanic and continental plates in the Pacific basin, *Spec. Pap. Geol. Soc. Am., 205*, 59 pp., 1985.

Fisher, R. A., Dispersion on a sphere, *Proc. R. Soc. London, 217*, 295–305, 1953.

Fitch, T. J., Plate convergence, transcurrent faults, and internal deformation adjacent to southeast Asia and the western Pacific, *J. Geophys. Res., 77*, 4432–4460, 1972.

Fox, K. F., R. J. Fleck, G. H. Curtis, and C. E. Meyer, Implications of the northwestwardly younger age of the volcanic rocks of west-central California, *Geol. Soc. Am. Bull., 96*, 647–654, 1985.

Frizzell, V. A., Jr., and M. L. Zoback, Stress orientation determined from fault slip data in Hampel Wash area, Nevada, and its relation to contemporary regional stress field, *Tectonics, 6*, 89–98, 1987.

Graham, S. A., and W. R. Dickinson, Evidence for 115 kilometers of right slip on the San Gregorio-Hosgri fault trend, *Science, 199*, 179–181, 1978.

Harden, D. R., H. M. Kelsey, T. A. Stephens, and S. Morrison, Geologic map of the Redwood Creek basin, *U.S. Geol. Surv. Water Resour. Div. Open File Rep., 81-496*, 1982.

Harding, T. P., Newport-Inglewood trend, California—An example of wrench style of deformation, *Am. Assoc. Pet. Geol. Bull., 56*, 97–116, 1973.

Harsh, P. W., E. H. Pampeyan, and J. M. Oakley, Slip on Willits fault, California (abstract), *Earthquake Notes, 49*, 22, 1978.

Heaton, T. H., and S. H. Hartzell, Earthquake hazards on the Cascadia subduction zone, *Science, 236*, 162–168, 1987.

Herd, D. G., Intracontinental plate boundary east of Cape Mendocino, *Geology, 6*, 721–725, 1978.

Hobbs, B. E., W. D. Means, and P. F. Williams, *An Outline of Structural Geology*, 571 pp., John Wiley, New York, 1976.

Jachens, R. C., and A. Griscom, Three-dimensional geometry of the Gorda plate beneath northern California, *J. Geophys. Res., 88*, 9375–9392, 1983.

Jarrard, R. D., Terrane motion by strike-slip faulting of forearc slivers, *Geology, 14*, 780–783, 1986.

Jennings, C. W. (Compiler), Geologic map of California, scale 1:750,000: Calif. Div. of Mines and Geol., Sacramento, 1977.

Jones, D. L., M. C. Blake, Jr., E. H. Bailey, and R. J. McLaughlin, Distribution and character of upper Mesozoic subduction complexes along the west coast of North America, *Tectonophysics, 47*, 207–222, 1978.

Kelsey, H. M., and A. O. Allwardt, Evidence for a major Quaternary fault zone in the Central Belt Franciscan melange, northern California (abstract), *Geol. Soc. Am. Abstr. Programs, 15*, 316, 1983.

Kelsey, H. M., and S. M. Cashman, Wrench faulting in northern California and its tectonic implications, *Tectonics, 2*, 565–576, 1983.

Kelsey, H. M., and D. K. Hagans, Major right-lateral faulting in the Franciscan assemblage of northern California in late Tertiary time, *Geology, 10*, 387–391, 1982.

MacGinitie, H., Central and southern Humboldt County, *Bull. Calif. Div. Mines Geol., 118*, 643–645, 1943.

Manning, G. A., and B. A. Ogle, Geology of the Blue Lake Quadrangle, California, *Bull. Calif. Div. Mines Geol., 148*, 35 pp., 1950.

McEvilly, T. V., Sea floor mechanics north of Cape Mendocino, California, *Nature, 220*, 901–903, 1966.

McKenzie, D. P., and W. J. Morgan, Evolution of triple junctions, *Nature, 224*, 125–133, 1969.

McLaughlin, R. J., The Sargent-Berrocal fault zone and its relation to the San Andreas fault system in the southern San Francisco bay region and Santa Clara Valley, California, *J. Res. U.S. Geol. Surv., 2*, 593–598, 1974.

McLaughlin, R. J., and T. H. Nilsen, Neogene non-marine sedimentation and tectonics in small pull-apart basins of the San Andreas fault system, Sonoma County, California, *Sedimentology, 29*, 865–876, 1982.

McLaughlin, R. J., S. A. Kling, R. Z. Poore, K. L. McDougall, and E. C. Beutner, Post-middle Miocene accretion of Franciscan rocks, northwestern, California, *Geol. Soc. Am. Bull., 93*, 595–605, 1982.

McLaughlin, R. J., H. N. Ohlin, D. J. Thormahlen, D. L. Jones, J. W. Miller, and C. D. Blome, Geologic map and structure sections of the Little Indian Valley-Wilbur Springs geothermal area, northern Coast Ranges, California, *U.S. Geol. Surv. Open File Rep., 85-285*, 24 pp. and two map sheets, 1985*a*.

McLaughlin, R. J., D. H. Sorg, J. L. Morton, T. G. Theodore, and C. E. Meyer, Paragenesis and tectonic significance of base and precious metal occurrences along the San Andreas fault at Point Delgada, California, *Econ. Geol., 80*, 344–359, 1985*b*.

McPherson, R. C., S. W. Smith, and N. I. Severy, The Humboldt Bay seismic network, 1974–1980 (abstract), *Earthquake Notes, 52*, 41, 1981.

Menack, J. S., Geology of the Neogene sedimentary rocks in Garberville, California, M.A. thesis, 231 pp., Cornell Univ., Ithaca, N.Y., June 1986.

Menack, J. S., B. Roth, and J. Barron, Tertiary terrane tectonics of northwestern California constrained by timing of Neogene shelf deposits (abstract), *Eos Trans. AGU, 66*, 1090, 1985.

Norris, R. J., and A. F. Cooper, Small-scale fractures, glaciated surfaces and recent strain adjacent to the Alpine fault, *Geology, 14*, 687–690, 1986.

Ogle, B. A., Geology of the Eel River Valley area, Humboldt County, California, *Bull. Calif. Div. Mines, 164*, 128 pp., 1953.

Pampeyan, E. H., P. W. Harsh, and J. M. Coakley, Preliminary map showing recently active breaks along the Maacama fault zone between Laytonville and Hopland, Mendocino County, California, *U.S. Geol. Surv. Map, MF-1217*, 1981.

Prescott, W. H., and S. Yu, Geodetic measurement of horizontal deformation in the northern San Francisco Bay region, California, *J. Geophys. Res., 9*, 7475–7484, 1986.

Raff, A. D., and R. G. Mason, Magnetic survey off the west coast of North America, 40°N latitude to 50°N latitude, *Geol. Soc. Am. Bull., 72*, 1267–1270, 1961.

Riddihough, R., Recent movements of the Juan de Fuca plate system, *J. Geophys. Res., 89*, 6980–6994, 1984.

Sarna-Wojcicki, A. M., S. D. Morrison, C. E. Meyer, and J. W. Hillhouse, Correlation of upper Cenozoic tephra layers between sediments of the western United States and eastern Pacific Ocean and

comparison with biostratigraphic and magnetostratigraphic age data, *Geol. Soc. Am. Bull.*, *98*, 207–223, 1987.

Sibson, R. H., Earthquakes and linear infrastructure, *Philos. Trans. R. Soc. London, Ser. A*, *317*, 63–79, 1986.

Silver, E. A., Tectonics of the Mendocino triple junction, *Geol. Soc. Am. Bull.*, *82*, 2965–2978, 1971.

Simila, G. W., Seismological evidence on the tectonics of the northern section of the San Andreas fault region, Studies of the San Andreas Fault Zone in Northern California, edited by R. Streitz and R. Sherburne, *Spec. Rep. Calif. Div. Mines Geol.*, *140*, 131–138, 1980.

Simila, G. W., W. A. Peppin, and T. V. McEvilly, Seismotectonics of the Cape Mendocino, California, area, *Geol. Soc. Am. Bull.*, *86*, 1399–1406, 1975.

Smith, S. W., and J. S. Knapp, The northern termination of the San Andreas fault, Studies of the San Andreas Fault Zone in Northern California, edited by R. Streitz, and R. Sherburne, *Spec. Rep. Calif. Div. Mines Geol.*, *140*, 153–164, 1980.

Smith, S. W., R. C. McPherson, and N. I. Severy, The Eureka earthquake of 1980, breakup of the Gorda plate (abstract), *Earthquake Notes*, *52*, 44, 1981.

Snay, R. A., M. W. Cline, and E. L. Timmerman, Project REDEAM: Models for historical horizontal deformation, *NOAA Tech. Rep., NOS 125 NGS 42*, 76 pp., 1987.

Suppe, J., *Principles of Structural Geology*, 537 pp., Prentice-Hall, Englewood Cliffs, N. J., 1985.

Underwood, M. B., The Garberville thrust—A contact of probably Miocene age within the Franciscan Complex, northern California (abstract), *Geol. Soc. Am. Abstr. Programs*, *14*, 635–636, 1982.

Upp, R. R., Holocene activity on the Maacama fault, Mendocino County, California, Ph.D. thesis, 112 pp., Stanford Univ., Stanford, Calif., 1982.

Vink, G. E., W. J. Morgan, and W. Zhao, Preferential rifting of continents: A source of displaced terranes, *J. Geophys. Res.*, *89*, 10,072–10,076, 1984.

Wagner, D. L., and E. J. Bortugno, Geologic map of the Santa Rosa quadrangle, scale 1:250,000, map 2A, 5 sheets, Calif. Div. of Mines and Geol., Reg. Geol. Map Serv., Sacramento, 1982.

Walter, S. R., Intermediate-focus earthquakes associated with Gorda plate subduction in northern California, *Bull. Seismol. Soc. Am.*, *76*, 583–588, 1986.

Wilcox, R. E., T. P. Harding, and D. R. Seeley, Basic wrench tectonics, *Am. Assoc. Pet. Geol. Bull.*, *557*, 74–96, 1973.

Wilson, D. S., A kinematic model for the Gorda deformation zone as a diffuse southern boundary of the Juan de Fuca plate, *J. Geophys. Res.*, *91*, 10,259–10,270, 1986.

Woodward-Clyde Associates, Evaluation of the potential for resolving the geologic and seismic issues at the Humboldt Bay Power Plant Unit no. 3, appendices, Woodward-Clyde Consultants, Walnut Creek, Calif., 1980.

Wright, R. H., D. H. Hamilton, T. D. Hunt, M. L. Traubenik, and R. J. Shlemon, Character and activity of the Greenville structural trend, Proceedings, Conference on Earthquake Hazards in the Eastern San Francisco Bay Area, edited by E. W. Hart, S. E. Hirschfeld, and S. S. Schulz, *Spec. Publ. Calif. Div. Mines Geol.*, *62*, 187–196, 1982.

G. A. Carver, Department of Geology, Humboldt State University, Arcata, CA 95521.

H. M. Kelsey, Department of Geology, Western Washington University, Bellingham, WA 98225.

(Received June 19, 1987;
revised January 7, 1988;
accepted November 12, 1987.)